CHARACTERIZATION OF MEMORY CYTOTOXIC T LYMPHOCYTE RESPONSES IN CHRONIC HIV-1 INFECTED INDIVIDUALS

by

Yunhan Jiang

BS Soochow University, China, 2015

Submitted to the Graduate Faculty of

Graduate School of Public Health in partial fulfillment

of the requirements for the degree of

Master of Science

University of Pittsburgh

2017

UNIVERSITY OF PITTSBURGH

Graduate School of Public Health

This thesis was presented

by

Yunhan Jiang

It was defended on

April 13th, 2017

and approved by

Thesis Advisor:
Paolo A Piazza, PhD
Research Assistant Professor
Infectious Diseases and Microbiology
Graduate School of Public Health
University of Pittsburgh

Committee Members:

Charles R Rinaldo, PhD
Professor and Chair
Infectious Diseases and Microbiology
Graduate School of Public Health
University of Pittsburgh

Nicolas Sluis-Cremer, PhD
Associate Professor and Director of Laboratory Research
Division of Infectious Diseases
Department of Medicine
University of Pittsburgh

Paolo A Piazza, PhD

CHARACTERIZATION OF MEMORY CYTOTOXIC T LYMPHOCYTE RESPONSES IN CHRONIC HIV-1 INFECTED INDIVIDUALS

Yunhan Jiang, MS

University of Pittsburgh, 2017

ABSTRACT

The three stages of untreated human immune deficiency virus type 1 (HIV-1) infection are acute HIV infection, chronic HIV infection, and acquired immunodeficiency syndrome (AIDS). Combination antiretroviral therapy (cART) is effective in treating chronic HIV infection but fails to completely clear the virus. Mutations in HIV epitopes recognized by cytotoxic T lymphocytes (CTL) could be a major contributing factor because they result in T cell mediated immune responses with limited effectiveness. In the absence of cART, it is the viral evolution within an individual during the course of infection under the pressure of host immune response that allows the virus to persist. To better understand viral pathogenesis and develop an effective HIV treatment, it is important to identify and characterize the evolution of mutations occurring within HIV CTL epitopes.

Here I mapped the evolution of HIV CTL epitopes in chronically infected HIV-1 donors. Specifically, I fist 1) identified memory HIV CTL epitopes to HIV *gag* antigens p17/p24 from contemporaneous viral isolates obtained from long term HIV infected individuals and then 2) compared CTL responses to epitope sequences from the early stages of infection versus sequences after over 10 years of treatment and viral evolution. Using MHC class-1 binding predictive algorithm, the viral mutation was found to exhibit an unexpected pattern, that the reservoir variants has a higher binding affinity than its founder variant. Making use of an IFN-γ ELISpot Assay, the

fact that the MHC class-1 binding affinity does not equal to the actual elicited CTL response has been noticed.

Overall, this study has a significance in public health as it provided important information on the ability of HIV to escape $CD8^+$ T lymphocyte detection and potentially contribute to the cure of the disease.

TABLE OF CONTENTS

LIST OF TABLES

LIST OF FIGURES

PREFACE

First and foremost, I appreciate my advisor, Dr. Paolo A Piazza, for his guidance on my research and thesis writing. Second, I would like to express my heartfelt gratitude to Dr. Robbie Mailliard for his support not only on my research and study but also on my career development. I want to thank my committee members Dr. Charles R Rinaldo and Dr. Nicolas Paul Sluis-Cremer for their advice on this thesis. My sincere thanks also go to Dr. Mariana Palma, Dr. Tatiana Garcia-Bates, Pranali Ravikumar, Diana Campbell, Kathleen Hartle, Janet L Mclaughlin, Angela Anthony, Jan Kristoff for their generous advises and help.

Finally, I want to thank my parents Mr. Shichang Jiang and Mrs. Jianying Yang for supporting me spiritually and great confidence in me all through these years.

1.0 INTRODUCTION

The Human Immunodeficiency Virus (HIV) is a lentivirus that causes HIV infection. HIV can be divided into two major types, HIV type 1 (HIV-1) and HIV type 2 (HIV-2). HIV-1, however, is the most common and pathogenic strain. Without treatment, HIV-1 infection progresses through three stages: acute HIV infection, chronic infection, and acquired immunodeficiency syndrome (AIDS) as the result of a gradual destruction of the $CD4^+$ T cells.

Currently there is no cure for HIV-1 infection that results in complete elimination of the virus. Combination antiretroviral therapy (cART) is medications that currently used to treat HIV-1 infection. It consists of a combination of drugs that are used to prevent the growth of the virus and keep HIV infection under control. Although cART has shown its effectiveness in preventing the development of AIDS and has led to a significant recovery of $CD4^+$ T cells in the majority of recipients, it does not lead to complete clearance of HIV.

The cytotoxic T lymphocyte (CTL) is regarded as one of the major effector cell types acting upon viral infection [1, 2]. However, a diminished killing capacity of the CTLs from chronic HIV-1 infected individuals has been observed [3]. Under the pressure of the host immune response in chronically infected individuals, viral mutations may arise in HIV-1 CTL epitopes which could be the major contributing factor that enables the virus to persist. Identifying mutations within these HIV-1 epitopes and characterizing the functional immune response in vitro following their

evolution in the host, could contribute to a better understanding of viral pathogenesis and develop an effective treatment for the eradication of HIV-1 infection.

1.1 HUMAN IMMUNODEFICIENCY VIRUS (HIV)

1.1.1 Epidemiology

HIV infects and kills cells of the immune system to cause a progressive and ultimately fatal immunodeficiency in humans and it has been a major burden on society since it emerged over 30 years ago [4]. According to the WHO, there were approximately 36.7 million people around the world living with HIV at the end of 2015, among which 2.1 million people are newly infected. Around 1.1 million people died from AIDS in year 2015.

HIV can be divided into two major types, HIV type 1 (HIV-1) and HIV type 2 (HIV-2). HIV-1 primarily originated from gorillas and chimpanzees in West Africa, while HIV-2 was originally discovered in endangered west African primate sooty mangabey [5]. HIV-1 is the most common and pathogenic of the two viruses and is the cause of the majority of HIV infections globally, whereas HIV-2 infections are mainly seen only in a few west African countries because of its relatively poor capacity for transmission [6].

1.1.2 Viral Structure

HIV is a lentivirus, a subgroup of retroviruses [7]. Mature HIV virions have spherical morphology of 100–120 nm in diameter [8]. The virus structure mainly consists of three parts: the

viral envelope, the viral matrix proteins and the viral core. The viral envelope is the outer coat of the virus and is made up of two layers of phospholipids, where three transmembrane glycoprotein gp41 are embedded each one attached to one molecule of the surface glycoprotein (gp) 120. Both gp120 and gp41 are encoded by the *env* gene of the viral RNA genome and they are critical for the viral attachment and cell fusion processes. The matrix protein p17 lies between viral envelope and core. The core proteins consisting of capsid protein p24, late assembly protein p6 and nucleocapsid protein p7 which is bound to the RNA genome. They are all encoded by the viral *gag* gene. Within the viral core, there are two copies of positive-sense viral RNA genome, each around 10 kb in length, and which are associated together with the protease, integrase and reverse transcriptase enzymes. These three enzymes are encoded by the viral *pol* gene. As *gag* proteins of HIV-1 are central players in virus particle assembly, release, and maturation, and also function in the establishment of a productive infection [9], they are highly expressed and relatively conserved in sequence due to overall fitness and survival. It has also been reported that *gag*-targeted CTLs are intrinsically superior to *env*-targeted CTLs, perhaps due to specific protein property such as early epitope presentation [10]. So *gag* protein is widely used in HIV-1 immunity research including vaccine development.

1.1.3 Pathogenesis and Host Response

Without treatment, HIV infection progresses in three stages: acute HIV infection, chronic HIV infection, and acquired immunodeficiency syndrome (AIDS). Acute infection, also called primary infection, generally develops within 2 to 4 weeks after the initial HIV exposure. During this time, 50-90% of infected individuals develop an influenza or mononucleosis-like illness which may last for a few weeks [11, 12]. The main target of HIV infection is activated $CD4^+$ T

lymphocytes. Viral entry occurs via interactions between *env* gp41 and gp120 on the virus particles and CD4 molecule and the chemokine co-receptors CCR5 or CXCR4. The distribution of these receptors on a variety of cell types central to the immune system permits infection not only limited to $CD4^+$ T lymphocytes, but also monocytes, macrophages and dendritic cells [13, 14]. In the early days of the acute infection stage, HIV replicates quickly within infected cells, which leads to a first increase in HIV RNA copies and a sharp decline in $CD4^+$ cells in the blood. When the host's anti-HIV adaptive immune response begins at 4 to 8 weeks after infection, symptoms of seroconversion may develop and viral load drops. The second stage of HIV infection is chronic HIV infection (also known as asymptomatic HIV infection or clinical latency). Patients with chronic HIV infection may not have any HIV-related symptoms. During this stage, the concentration of $CD4^+$ cell in the peripheral blood recovers, although not as high as it was before infection, and HIV-1 RNA copy number in the plasma declines again. Without treatments, it usually takes more than 10 years for chronic HIV-1 infection to progress to AIDS. AIDS is the final stage of HIV infection when the continuous destruction of $CD4^+$ T cells over years leads to a weakened immune system. Finally, the gradually weakened immune system eventually leaves the host vulnerable to serious infections and cancers that the host is barely capable to fight off. According to the CDC, people with AIDS typically survive about 3 years without treatment.

1.1.4 HIV-1 Treatment

The combination antiretroviral therapy (cART) identifies the medications regimen that is currently used to treat HIV infection. It consists of a combinations of drugs that are used to prevent the growth of the virus and keep HIV-1 infection under control, such as Combivir™ (GlaxoSmithKline Ltd, Brentford Middlesex, UK) is a combination of two Nucleoside Reverse

Transcriptase Inhibitors (NRTIs), azidothymidine (zidovudine, 3'-Azido-3'-deoxythymidine, AZT) which is a thymidine analogue, and lamivudine (2'-Deoxy-3'-thiacytidine, 3TC), which a cytosine analogue [15]; Truvada™ (Gilead Sciences Inc, Foster City, CA, US) is a combination of two NRTIs [16], emtricitabine (2'-deoxy-5-fluoro-3'thiacytidine, FTC) which is a cytidine analogue, and tenofovir disoproxil fumarate (TDF) which is a adenine analogue.

However, although cART results in near complete suppression of HIV-1 replication and a significant recovery of the peripheral $CD4^+$ T cell compartment in the majority of recipients, it does not lead to a clearance of the viral load. Once the treatment was interrupted, the viral load rebounds again followed by a decline of $CD4^+$ T cells. As a result, the treatment has to be lifelong.

The main obstacle to curing HIV-1 is the latency, which is defined as the persistence of integrated viral DNA that is replication competent but transcriptionally silent [17]. The latent HIV reservoir is established typically in resting $CD4^+$ T cells [18-21]. These cells have viral DNA integrated in their chromosomes but express little or no viral RNA and no viral proteins, which make them beyond the reach of cART and substantially invisible to the immune system. However, these cells can produce infectious virus once they were stimulated; thus, they can restart virus replication if a patient discontinues cART. In addition to serving as a persistent source of virus, the latent reservoir can also serve as an archive of viral variants, which challenges the clearance of virus for it could maintain drug-resistant and CTL-resistant variants [22].

1.2 IMPORTANCE OF ANTIGEN PRESENTING CELL

Activation of specialized antigen presenting cells (APCs) is a necessary first step for induction of adaptive immunity. They are a class of cells that can uptake, process and present

antigen information to T lymphocytes. The dendritic cell (DC) is known as the professional antigen present cell among all other cells. DC populate most tissues in the body, play an important role in surveillance and homeostasis and serve as the initiator of adaptive immune responses by establishing the bridges linking innate and adaptive immunity. Upon infection, antigen captured by recognition of pathogen-associated molecular patterns (PAMPs) via pattern recognition receptors (PRRs), expressed at the surface of DCs, triggers the maturation process, leading to DC migration to draining lymph nodes, where they present antigens to T cells. Thus, naïve $CD4^+$ T cells got primed and polarized into various Th phenotypes [23], viral antigen got presented to $CD8^+$ T cells. Interestingly, previous research has also shown that DCs plays an important role in viral dissemination and immune dysregulation associated with HIV infection [24, 25]. Nevertheless, all these previous studies have shown that professional APC, especially DCs, are vital for an efficient immune response upon pathogen infection.

The maturation status of DC is important to DC function, due to changes in the surface expression and secretion of several proteins. For convenience, most laboratory protocols that employ dendritic cells start from blood derived $CD14^+$ monocytes: these are isolated from peripheral blood mononuclear cells (PBMCs) and differentiated in immature DCs (iDCs) using granulocyte macrophage colony-stimulating factor (GM-CSF) and interleukin-4 (IL-4), though some people use interferon-α (IFN-α) instead of IL-4 [26]. These iDCs have high antigen capture capacity. There are various protocols for DC maturation from immature precursors. Factors used to mature immature DCs included lipopolysaccharide (LPS) [27-32], CD40 ligand (CD40L) [33, 34], tumor necrosis factor-α (TNF-α) [26], IFN-α [35] and IFN-γ [36, 37]. To create a better inflammatory environment, different cocktails of maturation inducing factors have also been used. The maturation cocktail including interleukin-1β (IL-1β), TNF-α, IL-6 and prostaglandin E2

(PGE2) [38] was regarded as the "gold-standard" for its capacity to induce highly efficient mature DCs (which will be termed "DC2" from here on in this manuscript). However, more recent studies have shown that DCs matured with this protocol (DC2) display a reduced ability to secrete active interleukin-12p70 (IL-12p70) [39], which is known to induce enhancement of the cytotoxic activity of NK cells and CTLs. IL-12p70 also plays a role in the development of cytotoxicity of activated $CD8^+$ T cells as well as promoting the production of IFN-γ [40]. In the absence of IL-12, $CD8^+$ T cells failed to express granzyme B and thus lack cytolytic function [41]. DCs matured by another maturation cocktail including IFN-γ, IFN-α, TNF-α, IL-1β and polyinosinic: polycytidylic acid (poly (I:C) and which will be termed "αDC1" from here on in this manuscript, have shown migratory responsiveness to various chemokines, and most importantly, have high IL-12p70-producing ability compared to DC2 [42]. Though various protocols has been reported for DC maturation, it still remains unclear which one provides the optimal DCs for *in vitro* immune response activation and only a few have been widely tested in clinical trials [43].

1.3 CELL-MIDIATED IMMUNE RESPONSE TO HIV-1

After the pathogen got recognized by APCs, exogenous antigens were presented to T helper cells ($CD4^+$) by the use of MHC class II molecules on their surface, whereas endogenous antigens were presented on the cell surface in the complex with MHC class I molecules which activated CTLs. Cytotoxic T lymphocytes (CTLs), or $CD8^+$ T lymphocytes, are the major responder cell type in the adaptive immune response to viruses. The killing efficiency of CTL is critical for the control of HIV-1 infection [44]. They played an important role in suppressing HIV-1 replication during acute infection [45-47]. However, CTL will also exert a strong selective pressure on the

virus, forcing HIV-1 to mutate to evade CTL recognition [48, 49]. As a result, CTL escape variants will mutate quickly away from the founder sequence to reservoir variants. Previous research has shown that the mutated reservoir variants are more likely to be CTL escape epitopes [50], and that CTL escape epitopes accumulate as the epidemic progresses [51]. Therefore, the existence of mutated CTL-resistant viruses that have successfully become stablished in the reservoir can be considered a major barrier to viral eradication.

How HIV-1 mutations facilitate viral escape has been studies extensively. Among possible reasons is that the viral mutation within the CTL-recognition epitopes can 1) affect the antigen processing, 2) reduce the binding to the MHC class-I molecule, and 3) diminish the ability of T cell receptors to interact with the presented peptides in the p-MHC complex: all of these can completely eliminate the effectiveness of any HIV-1 memory CTL response that is specific for the original, founder virus sequence [52]. However, CTL escape mutations could also result in dysfunctional cross-reactive memory CTL responses by partial activation of TCR through "altered peptide ligand" (APL), thus providing an even more efficient way to advance virus dissemination: instead of totally bypassing the CTL response, these mutations can selectively promote the helper activity of the CTL while inhibiting their capacity to kill antigen expressing targets (Fig.1) [53].

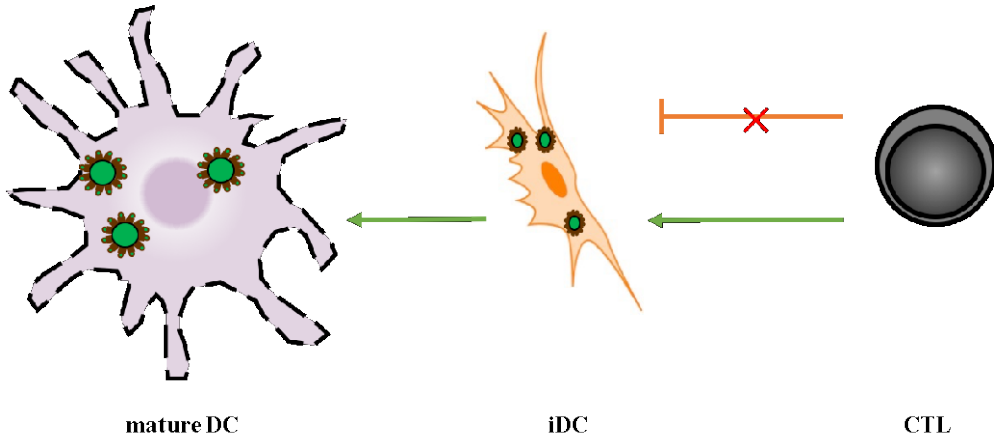

Figure 1. Viral 'Baiting' Strategy

When the CTL encounters HIV-1 variant APL epitopes on the surface of professional antigen presenting cells (pAPC) such as immature dendritic cells (iDC), instead of recognizing these iDC as infected targets ready for cytolysis and kill them, they provide signals that "help" activate the HIV-1 antigen presenting iDC, programming them to differentiate into a highly stimulatory, pro-inflammatory type of mature DC. These DC also rapidly sprout a web of micro- and nanotube-like extensions, allowing them to develop extensive interconnected cellular networks. HIV-1 may utilize such cellular connections for cell-to-cell spread and facilitate trans-infection of $CD4^+$ T cells [54, 55].

2.0 STATEMENT OF THE PROBLEM

There is no cure for HIV-1 infection. The current HIV-1 treatment combination antiretroviral therapy (cART) does not lead to clearance of the virus load. Viral mutations, specifically in epitopes recognized by CTL in chronic infected individuals during the course of infection and which are under the constant pressure of the host immune response could be the major contributing factor that enables the virus persist. However, how viral mutations facilitate viral escape is not completely elucidated. To better understand viral pathogenesis and develop an effective HIV treatment, it is important to identify the epitopes recognized by chronic HIV-1 infected individuals and compare the memory CTL responses against founder epitopes (i.e. HIV-1 CTL epitopes developed very early in the infection) versus reservoir epitopes (i.e. epitopes that have become fixed over years of treatment and viral evolution).

2.1 AIM 1: IDENTIFY THE EPITOPES RECOGNIZED BY MEMORY CD8$^+$ T CELLS IN SPECIFIC HIV-1 CHRONIC INFECTED INDIVIDUALS

Memory CD8+ T cells were re-stimulated with optimal autologous HIV-1 loaded mature dendritic cells. In order to identify the epitopes recognized by memory CD8$^+$ T cells, a synthetic peptide library of 18-mers each overlapping by 14 amino acids was generated representing the consensus HIV-1 *gag* p17 and p24 sequences during cART from each participant. The IFN-γ response of memory CD8$^+$ T cells to each 18-mer was tested by a IFN-γ Enzyme-Linked

ImmunoSpot (ELISpot) Assay. Groups of 18-mer peptides that induced a positive response were then defined as “hot spots”.

Having thus determined the antigenic hot spots, in order to identify the actual epitopes, I used the *Immune Epitope Database (IEDB) Analysis Resource* (http://tools.iedb.org/mhci/), which provides a collection of algorithms for the prediction and analysis of MHC binding epitopes [56, 57]. Combining the results from ELISpot and the predictive algorithm, I found several “potential epitopes”.

2.2 AIM 2: COMPARE MEMORY CTL RESPONSES AGAINST FOUNDER VARIANTS VERSUS RESERVOIR VARIANTS

To better understand the mechanisms of how viral mutations and CTL escape occur and evolve, the second aim is to measure, within each participant, the contemporaneous memory CTL response (specific for epitopes currently fixed in the reservoir) against the founder epitope variants and compare it against reservoir variants.

To focus on viral escape CTL epitopes, all the hot spots from 18-mer peptides that did not contain any mutation throughout the years were excluded, as they could not be escape epitopes by definition. These mutation including epitopes are therefore and hereon defined as the “candidate epitopes”. After alignment of the viral *gag* p17 and p24 sequence by years, all the founder and reservoir variants of “candidate epitopes” have been identified. Then a comparison on the CTL response against founder versus reservoir variants has been done using HLA binding predicted algorithm as well as a IFN-γ ELISpot Assay.

3.0 MATERIALS AND METHODS

3.1 STUDY PARTICIPANTS

The chronic HIV-1-infected participants (designated participants S4 and S5) were chosen from the Multicenter AIDS Cohort study (MACS), which is a prospective study of the natural and treated histories of HIV-1 infection in homosexual and bisexual men. The participants were chosen based on their prolonged enrollment in the study (over 10 years), their typical course of disease progression and their favorable response to combination antiretroviral therapy (cART) [58]. Both participants were enrolled in the MACS prior to HIV-1 seroconversion. Seropositivity was confirmed by an enzyme-linked immunosorbent assay (ELISA) positive for the presence of HIV-1 p24 and by Western blotting with bands corresponding to at least two of the *gag*, *pol*, and *env* proteins [59]. Blood specimens and epidemiological and clinical data were collected at each visit, as described previously [60].

3.2 CLINICAL AND VIROLOGIC CHARACTERISTICS

At each biannual visit, plasma samples and peripheral blood mononuclear cells (PBMC) were collected from the study participants and were stored at −80°C and −140°C, respectively. T cell phenotypes and HIV-1 plasma viremia were determined as previously described [61-63].

3.3 HIV-1 SEQUENCING AND PEPTIDE SYNTHESIS

Seven post-seroconversion (post-SC) time points and one post-cART time point for both participants S4 and S5 were chosen for HIV-1 *gag* p17-p24 sequencing and were sequenced from purified virus as described previously [63], and a peptide library of 18-mers overlapping by 14 amino acids was generated representing the consensus HIV-1 *gag* p17 and p24 sequences during cART from each participant. Potential variants for S4 were synthesized (Sigma-Aldrich) and were resuspended in dimethyl sulfoxide (DMSO) in a stock concentration of 10mg/ml. Peptides were further resuspended in AIM V medium at a using concentration of 100μg/ml. Peptides were stored at −80°C.

3.4 SEPARATION OF PBMC AND ISOLATION OF MONOCYTES

Contemporaneous PBMC from each study participant under cART were obtained by density gradient centrifugation using Ficoll-Paque (GE Healthcare Life Sciences, Uppsala, Sweden) and are stored at -140°C.

Monocytes were isolated using CD14 MicroBeads (Miltenyi Biotec, Bergisch Gladbach, Germany) following the product protocol.

3.5 GENERATION OF MONOCYTE-DERIVED DENDRITIC CELLS

Under stimulation of GM-CSF and IL-4 (both 1,000 U/ml, R&D Systems, Minneapolis, MN)), the monocytes will become immature DCs (iDCs) in Iscove's Modified Dulbecco's Medium (IMDM) containing 10% fetal bovine serum (FBS) at day 5 [42]. For DC stimulation, 0.5 million immature DCs were incubated with 50 ng of purified autologous aldrithiol-2 (AT-2)-inactivated HIV-1 for 2 h [64]. Immature DCs were then treated with two different cocktail of maturation factors:

- αDC1: IFN-γ (1000U/ml), IFN-α (3000U/ml), TNF-α (25ng/ml), IL-1β (25ng/ml), poly-I:C (20μg/ml).
- DC2: IFN-γ (1000U/ml), TNF-α (25ng/ml), IL-1β (25ng/ml), Il-6 (1000IU/ml), PEG2 (1mM).

DCs were then let develop into mature αDC1 and DC2 after 48 hours (Fig 2).

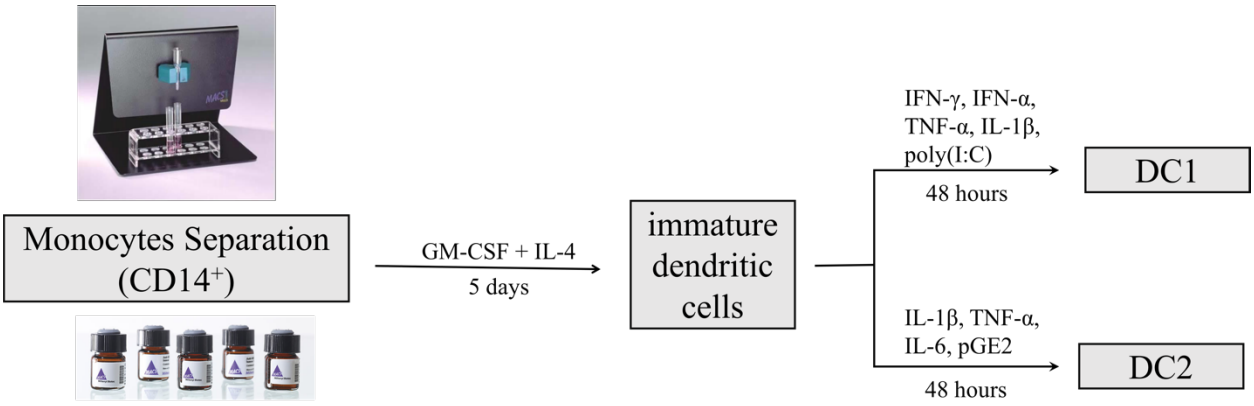

Figure 2. Flow chart of DC maturation

Monocytes were isolated from PBMC from each individuals and were developed into immature dendritic cells (iDCs) under the stimulation of GM-CSF and IL-4 at day 5. Based on the high antigen loading capacity iDCs, AT-2 inactivated autologous HIV-1 virus was added into iDCs at day 5 and incubated for 2 hours. Then the iDCs were

divided into two parts and two different cocktail of maturation factors were added into cells cultures individually. After 48 hours' incubation, the iDCs were developed into two types of mature DC, namely αDC1 and DC2.

3.6 DCS PHENOTYPING

The maturation status of αDC1 and DC2 were harvested and washed with PBS. Cells were then stained with CD83-PE (BD Pharmingen), CD86-PE (BD Pharmingen), or OX40L-PE (BD Pharmingen) for 20 minutes in room temperature respectively. Then cells were washed and fixed with 1% paraformaldehyde. The cell surface expression of CD83, CD86, and OX40L were analyzed on a BD LSR Fortessa flow cytometer using BD FACS Diva software. Data were analyzed by using FlowJo version 10.2.

3.7 IL-12P70 ELISA

Mature αDC and DC2 were harvested and washed thoroughly to remove all the cytokines. The cells were then plated at 2.5×10^4 cells/well in flat-bottomed 96-well plates. J558-CD40L cells were added at 5×10^4 cells/well and co-cultured with DCs for 24 hours. After incubation, the supernatants from each culture were harvested and were tested by ELISA for IL-12p70 to functionally characterize DCs.

3.8 RESTIMULATE MEMORY CTLS USING MATURE DCS

The two different types of mature DC were then combined with contemporaneous PBMC separated from the same study subject at 1:10 ratio respectively. The cultures were allowed to grow for 21 days and were supplemented with recombinant IL-2 (100 IU/ml), IL-7 (10 ng/ml) and IL-15 (2.5 ng/ml). After three weeks, specific epitopes recognized by memory CTLs were identified by IFN-γ ELISpot using the 18-mers peptide library. The entire work flow is shown in figure 3.

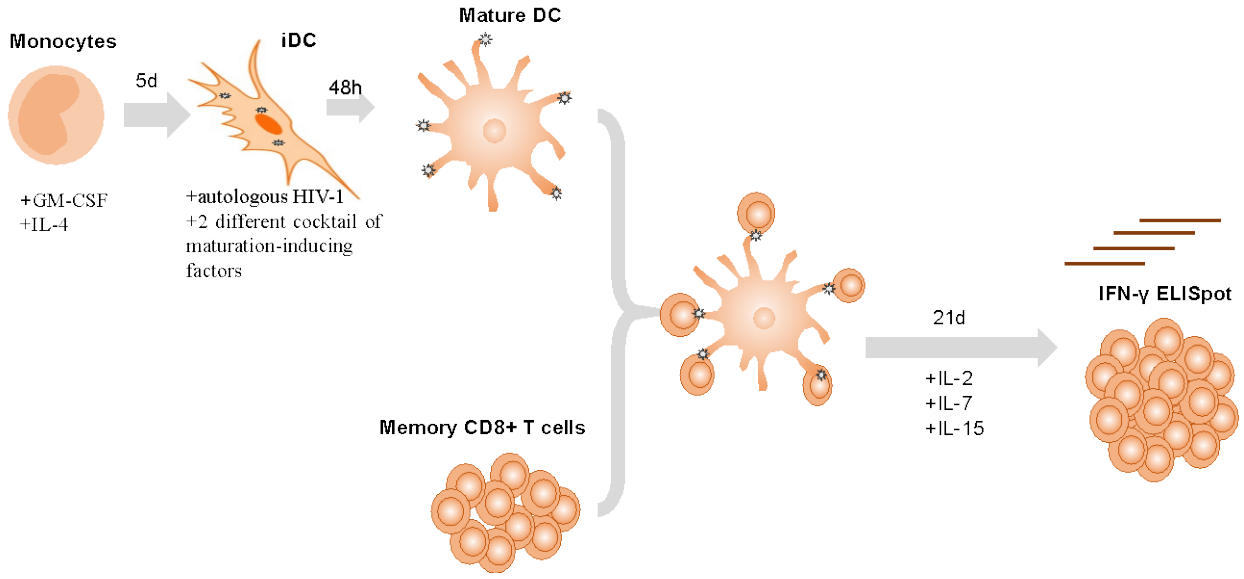

Figure 3. Flow chart of memory CD8⁺ T cell restimulation

Following stimulation with GM-CSF and IL-4, the monocytes will differentiate into immature DCs in 5 days. At day 5, autologous aldrithiol-2 (AT-2) [64] inactivated HIV-1 (the antigen) will be added to iDC into αDC1 and DC2 with two different cocktails of maturation factors. After 48 hours, mature DC are combined with autologous, frozen PBMC. Following a 21-day stimulation protocol, memory CD8⁺ T cells were evaluated for CTL effector function by IFN-γ ELISpot using the peptide library generated representing the consensus HIV-1 *gag* p17 and p24 sequences from each participant. Abbreviations: GM-CSF, granulocyte-macrophage colony-stimulating factor; IL-4, interleukin-4; IL-2,

interleukin-2; IL-7, interleukin-7; IL-15, interleukin-15; 5d, 5 days; 48h, 48 hours; 21d, 21 days; Mature, antigen-loaded DC (mature DC).

3.9 IFN-γ ELISPOT ASSAY

IFN-γ production was measured by a standard overnight enzyme-linked immunosorbent spot (ELISpot) assay. Briefly, 96-well Mixed Cellulose Esters (MCE) plates (EMD Millipore, Billerica, MA) were coated with anti-IFN-γ monoclonal antibody (10 μg/ml, Mabtech, Stockholm, Sweden) and incubated overnight at 4°C. At day 2, the plate was washed and blocked with IMDM supplemented with 10% heat-inactivated FBS for 2 h at 37°C. Memory CTLs were plated at 5×10^4 per well and the cells in duplicate wells were stimulated overnight at 37°C with each 18-mer peptide (10 μg/ml) in IMDM supplemented with 10% heat-inactivated FBS. At day 3, ELISpot plates were washed and processed as described previously [65, 66]. The spots were counted by an automated ELISpot plate reader (AID, Strasberg, Germany).

3.10 CD107A SURFACE STAINING ASSAY

Memory CTLs were harvested and stained with CD107a-FITC (BD Pharmingen) at the beginning of stimulation along with each interested 18-mer peptides. After overnight incubation at 37°C, cells were washed with PBS, surface stained with antibodies to CD3-APC-H7 (BD Pharmingen), CD4-V450 (BD Pharmingen), CD8-Percp-cy5.5 (BD Pharmingen) and Live/Dead Aqua Viability dye. Cells were washed and fixed in 1% paraformaldehyde. Flow cytometry gates for live, $CD3^+$,

CD4-, $CD8^+$, $CD107a^+$ were based on unstimulated control wells. Gating strategy is shown in Fig. 17.

4.0 RESULTS

4.1 THE MATURITY OF αDC1 AND DC2 FOR WAS CONFIRMED BY FLOW CYTOMETRY

For both study participant S4 and S5, the maturation status of αDC1 and DC2 was evaluated by extracellular staining using flow cytometry. The expression of CD83, CD86, and OX40Lwas evaluated. CD83 is a well-recognized marker for mature dendritic cells with regulatory function. CD86 is a protein expressed on antigen-presenting cells that provides costimulatory signals necessary for T cell activation and survival. OX40L controls the extent of T cell priming following recognition of antigen. Using Flow Cytometry, both αDC1 and DC2 showed a fully matured status with high expression of CD83, CD86 for either S4 (Fig.4) or S5 (Fig.5). OX40L expression is higher in DC2 than αDC1. This validate the use of either maturation factors to obtain DCs for memory $CD8^+$ T cells restimulation.

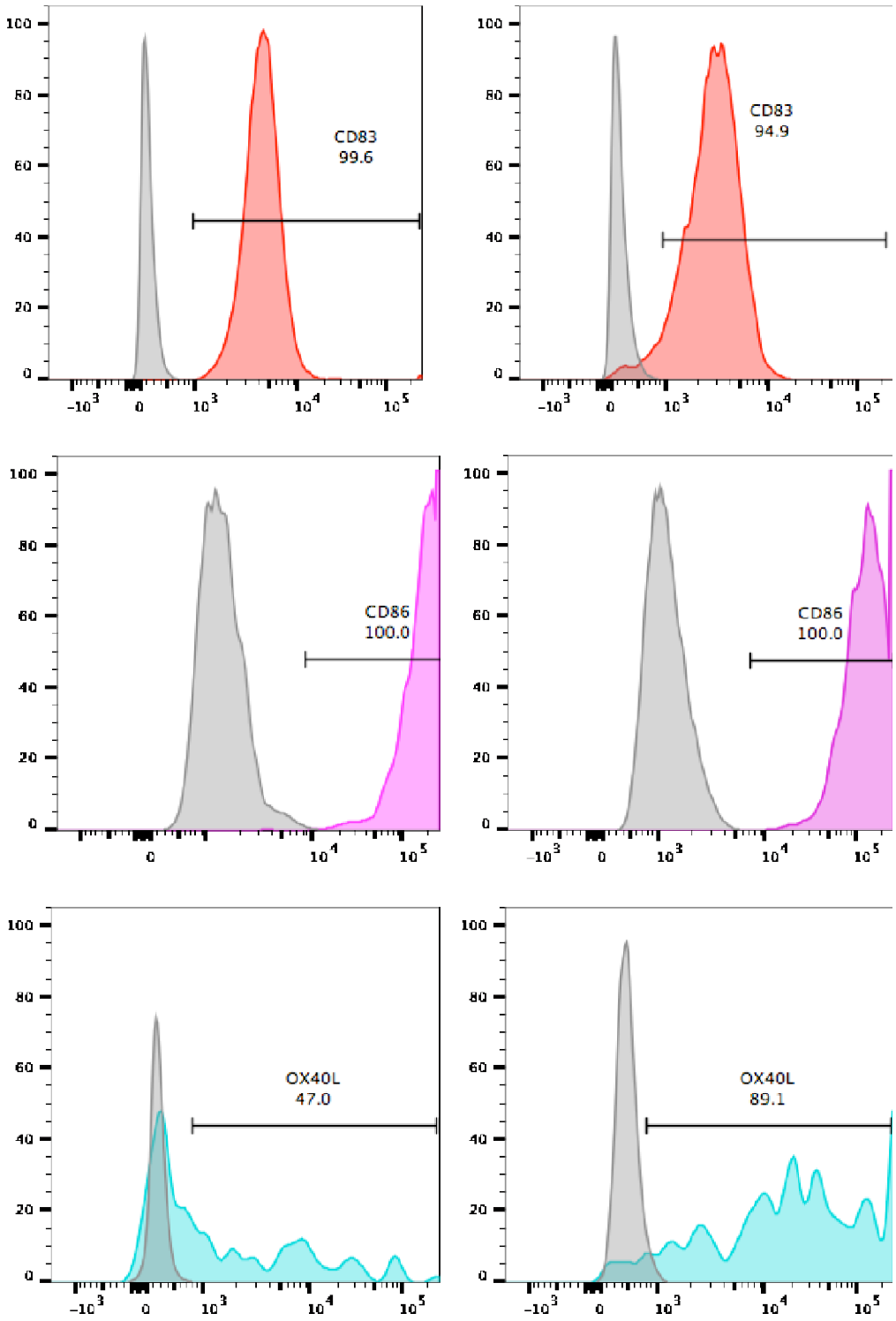

Figure 4. Both Mature αDC1 and DC2 for S4 can express high level of mature DC cell marker

The maturation status of αDC1 and DC2 for S4 was evaluated by flow cytometry staining for surface expression of CD83-PE, CD86-PE, and OX40L-PE. Left: αDC1. Right: DC2.

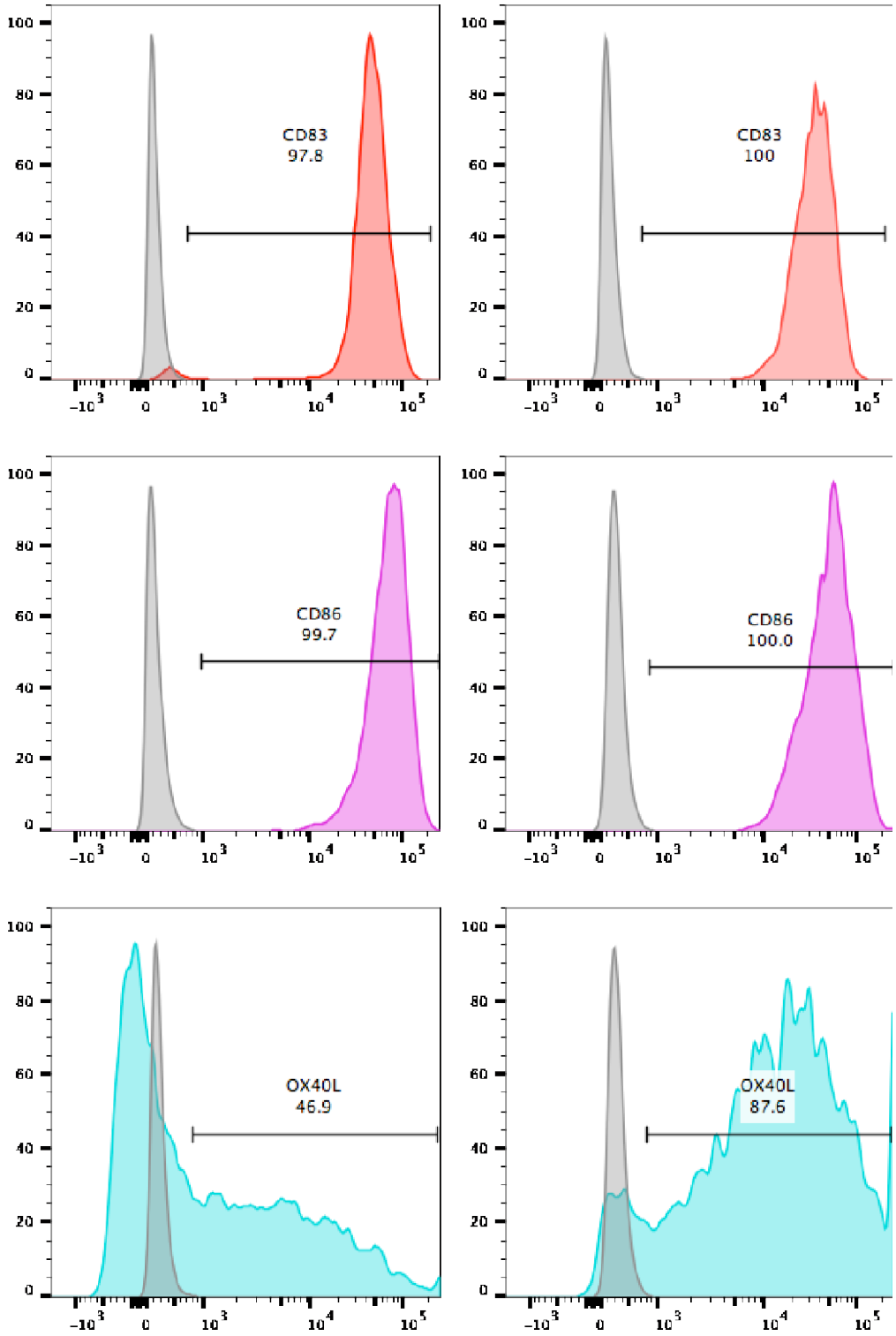

Figure 5. Both Mature αDC1 and DC2 for S5 can express high level of mature DC cell marker

The maturation status of αDC1 and DC2 for S5 was evaluated by flow cytometry staining for surface expression of CD83-PE, CD86-PE, and OX40L-PE. Left: αDC1. Right: DC2.

4.2 CYTOKINE PRODUCING ABILITY WAS EVALUATED FOR BOTH αDC1 AND DC2

The cytokine producing ability of S4 αDC1 and DC2 was determined using ELISA. Both mature αDC1 and DC2 were harvested and stimulated with CD40L. The IL-12p70 secreted by each group of cells were determined using ELISA.

Under CD40L stimulation, αDC1 produced around 10-fold IL-12p70 as of DC2 (Fig.6). This result indicates αDC1 could be a better choice for memory $CD8^+$ T cells restimulation.

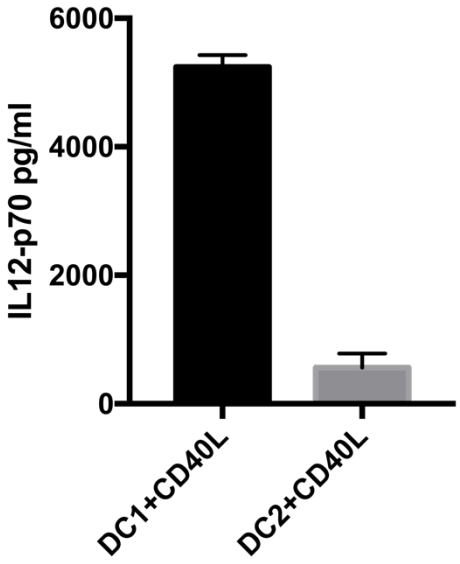

Figure 6. Mature αDC1 produce higher IL-12p70 amounts than DC2

Mature αDC1 and DC2 were harvested and co-cultured with J558-CD40L cells for 24 hours respectively. After 24 hours, supernatant from each culture was collected and the amount of IL-12p70 was determined using ELISA.

4.3 ANTIGEN LOADED αDC1 INDUCE A HIGHER MEMORY CTL RESPONSE THAN ANTIGEN LOADED DC2

To identify the specific epitopes recognized by CTL for each individual, we first generated the peptide library representing the consensus HIV-1 *gag* p17 and p24 sequences for each participant.

For participant 4 (S4), using mature αDC1 and DC2, I stimulated memory CTLs for 21 days with IL-2, IL-7 and IL-15 supplementation. After three weeks, the individual 18-mer peptides recognized by memory CTLs were identified by IFN-γ ELISpot. The results are shown as the number of net spot-forming cells (SFC) per 10^6 cells: these are "net" SFCs because the background from irrelevant peptide stimulated cultures was subtracted from the antigen-specific cultures (Fig.7). For S4, there are 28 18-mer peptides induced an IFN-γ CTL response that above the level when processed by αDC1, however, only 15 18-mer peptides when processed by DC2. The result indicates that αDC1 stimulated CTL can recognize a broader range of epitopes than DC2.

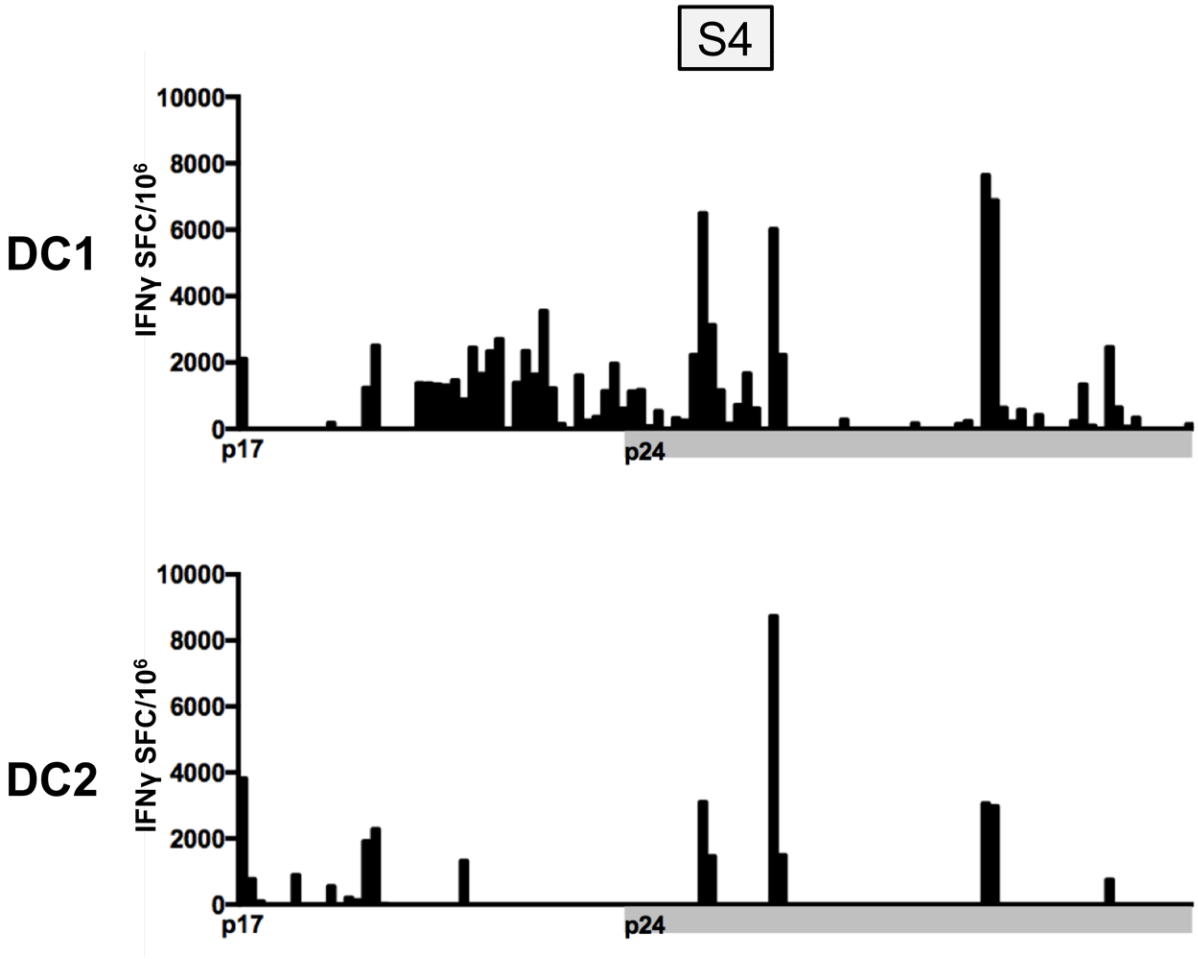

Figure 7. The "hot spots" for S4 were identified using IFN-γ ELISpot

The 18-mer recognized by S4 memory $CD8^+$ T cells were identified using IFN-γ ELISpot. The spots are shown as the number of background-subtracted antigen-specific spot-forming cells (SFC) per 10^6 cells. Background was calculated as the mean number of SFC/10^6 cells in duplicate control wells without peptide plus 2 standard deviations.

Then the responses of each peptide by αDC1 and DC2 were ranked in ascending order, respectively (Fig.8). The maximum response for αDC1 is 7,864 spots while for DC2 is 8,725 spots. Figure 8 shows that that αDC1 induce higher responses 1) on more peptides and 2) of higher sensitivities than DC2 do. Based on these findings, αDC1 were chosen to stimulate memory CTLs in all the following experiments.

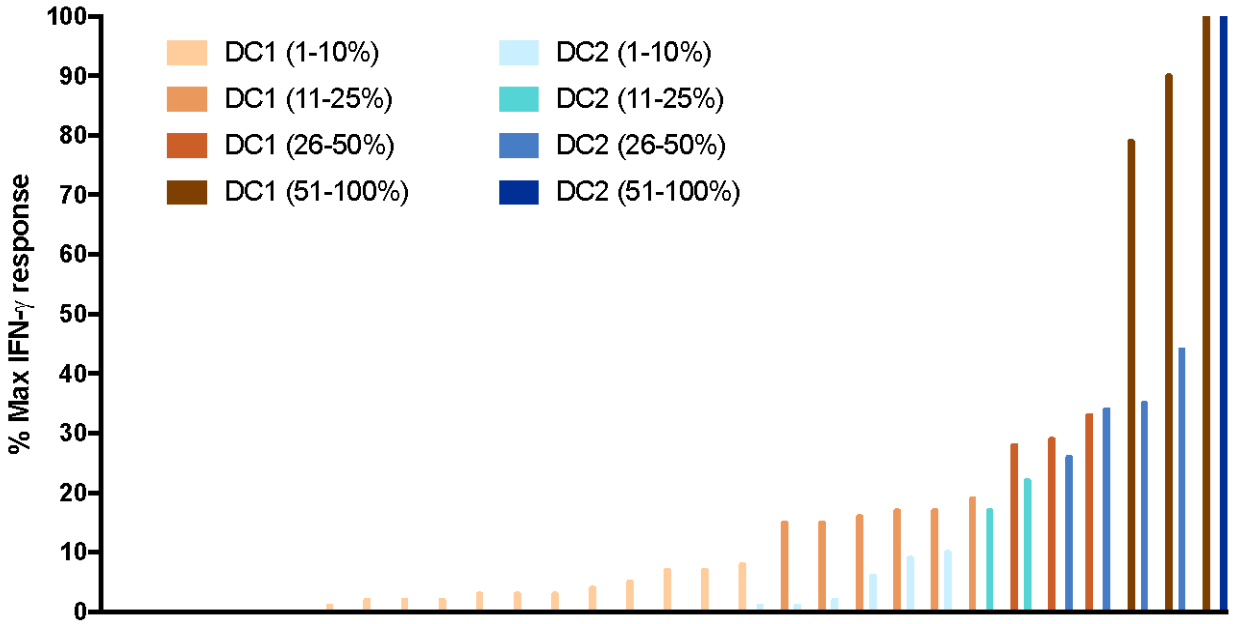

Figure 8. Comparison of memory CTL response stimulated by either αDC1 or DC2 based on the IFN-γ ELISpot assay

The CTL responses based on IFN-γ ELISpot assay was ranked compared to each maximum response. Orange: Memory $CD8^+$ T cells IFN-γ response stimulated by αDC1. Blue: Memory $CD8^+$ T cells IFN-γ response stimulated by DC2. IFN-γ ELISpot results were also ranked in four groups: group #1 number of responses between 1 and 10%, group #2 number of responses between 11and 25%, group #3 number of responses between 26 and 50%, group #4 number of responses between 51and 100% as t shown in the figure.

Similarly, S5 "hot spots" were determined following αDC1 stimulation of memory CTL using a library of overlapping 18-mer peptide corresponding to the contemporaneous autologous HIV-1 (Fig. 9).

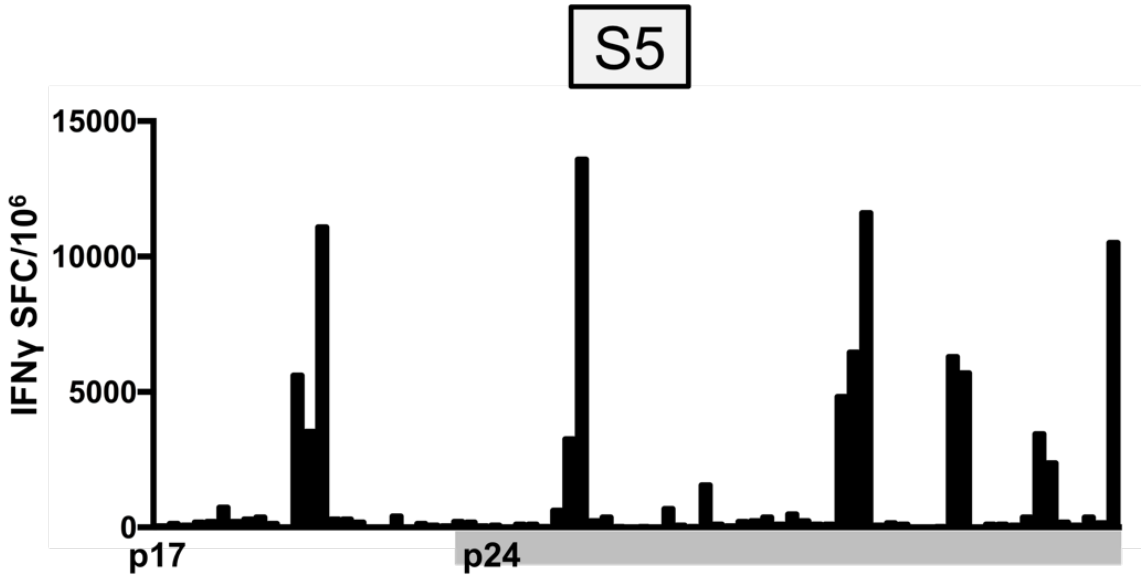

Figure 9. The "hot spots" for S5 were identified using IFN-γ ELISpot

The 18-mer recognized by S5 memory $CD8^+$ T cells were identified using IFN-γ ELISpot. The spots are shown as the number of background-subtracted antigen-specific spot-forming cells (SFC) per 10^6 cells. Background was calculated as the mean number of SFC/10^6 cells in duplicate control wells without peptide plus 2 standard deviations.

4.4 POTENTIAL EPITOPES ARE IDENTIFIED BASED ON IFN-γ ELISPOT RESONSES FOLLOWED BY MHC-1 BINDING PREDICTIVE ALGORITHM

As the 18-mer peptides are set up artificially, they are not the epitopes combined with MHC class I molecule and recognized by $CD8^+$ T cells. After I got the 18-mer "hot spots", I identified all the potential MHC class I-restricted epitopes for S4 and S5 by using predictive algorithm. The *Immune Epitope Database Analysis Resource* provides a collection of tools for the prediction and analysis of immune epitopes, which provides an access to predictions of peptide binding to MHC class I molecules. I have already known that the S4 MHC alleles are HLA-A*01:01, HLA-A*25:01, HLA-B*18:01, HLA-B*44:03, HLA-C*07:01, HLA-C*12:03, S5 MHC alleles are

HLA-A*02:01, HLA-A*26:02, HLA-B*15:01, HLA-B*44:02, HLA-C*03:04, HLA-C*15:01. The prediction method I used is artificial neural network (ANN) [67], which is a combination of several neural networks derived using different sequence-encoding schemes. The output is represented as IC50nM value. The lower the number of IC50nM value, the higher the potential binding affinity between peptide and MHC class I molecule. In general, most known epitopes have a IC50 that lower than 500nM. Using 500nM as a cut off, I got 99 predicted epitopes for S4 (Table 1) and 93 predicted epitopes for S5 (Table 2) that IC50nM lower than 500.

So far, the potential epitopes recognized by both study participant S4 and S5 $CD8^+$ T lymphocytes has been identified successfully.

Table 1. The predicted MHC class I-restricted epitopes for participant S4

participant	ID	18mer AA sequence	DC1-stimulated IFN-g SFC/10^6	MHC-1 restricted epitope AA sequence	Class 1 restriction	ic50
S4	73-1A	GKKKYQLKHIVWASRELE	2108	KHIVWASREL	HLA-C*07:01	61
				YQLKHIVWASREL	HLA-C*12:03	69
				KKYQLKHI	HLA-C*12:03	175
				YQLKHIVWASREL	HLA-C*07:01	315
				YQLKHIVW	HLA-C*12:03	362
				KKYQLKHIV	HLA-C*12:03	372
	73-11A	QSSLQTGSEEIKSLYNTV	168	GSEEIKSLY	HLA-A*01:01	47
				SEEIKSLY	HLA-B*44:03	184
				EEIKSLYNTV	HLA-B*44:03	280
				QTGSEEIKSLY	HLA-A*01:01	344
	73-15A	TVATLYCVHQKIEVKDTK	1228	TLYCVHQKI	HLA-C*12:03	248
				VATLYCVHQKI	HLA-C*12:03	310
				YCVHQKIEV	HLA-C*12:03	363
				TLYCVHQKIEV	HLA-C*12:03	434
	73-16A	LYCVHQKIEVKDTKEALD	2508	VHQKIEVKDTKEAL	HLA-C*07:01	194
				YCVHQKIEV	HLA-C*12:03	363
	73-23A	QNKAQQATAATGSSSQNYPI	1333	TAATGSSSQNYPI	HLA-C*12:03	177
				ATAATGSSSQNY	HLA-A*01:01	240
	73-24A	QATAATGSSSQNYPIVQNI	1293	QNYPIVQNI	HLA-C*12:03	53
				TAATGSSSQNYPIV	HLA-C*12:03	93
				TAATGSSSQNYPI	HLA-C*12:03	177
				ATAATGSSSQNY	HLA-A*01:01	240
	73-25A	TGSSSQNYPIVQNIQGQM	1453	QNYPIVQNI	HLA-C*12:03	53
				YPIVQNIQGQM	HLA-C*12:03	366
	73-26A	SQNYPIVQNIQGQMVHQA	1123	YPIVQNIQGQMV	HLA-C*12:03	28
				QNYPIVQNI	HLA-C*12:03	53
				QNYPIVQNIQGQMV	HLA-C*12:03	79
				YPIVQNIQGQM	HLA-C*12:03	366
				IVQNIQGQMV	HLA-C*12:03	408
	73-27A	NIQGQMVHQALSPRTLNA	1163	QALSPRTL	HLA-C*12:03	22
				VHQALSPRTL	HLA-C*07:01	36
				MVHQALSPRTL	HLA-C*12:03	120
	73-28A	QMVHQALSPRTLNAWVKV	73	QALSPRTLNAWVKV	HLA-C*12:03	21
				QALSPRTL	HLA-C*12:03	22
				VHQALSPRTL	HLA-C*07:01	36
				RTLNAWVKV	HLA-C*12:03	89
				MVHQALSPRTL	HLA-C*12:03	120
				QALSPRTLNAWV	HLA-C*12:03	233
	73-29A	QALSPRTLNAWVKVVEEK	533	QALSPRTLNAWVKV	HLA-C*12:03	21
				QALSPRTL	HLA-C*12:03	22
				RTLNAWVKVV	HLA-C*12:03	37
				RTLNAWVKV	HLA-C*12:03	89
				TLNAWVKVV	HLA-C*12:03	141
				LSPRTLNAWVKVV	HLA-C*12:03	232
				QALSPRTLNAWV	HLA-C*12:03	233
	73-32A	AMQMLKETINEEAAEWDR	6013	KETINEEAAEW	HLA-B*44:03	81
				MQMLKETI	HLA-C*12:03	128
	73-33A	LKETINEEAAEWDRLHPV	2223	EAAEWDRLHPV	HLA-C*12:03	18
				KETINEEAAEW	HLA-B*44:03	81
				NEEAAEWDRLHPV	HLA-B*18:01	112
				EAAEWDRL	HLA-C*12:03	144
	73-40	REPRGSDIAGTTSTLQEQ	273	IAGTTSTL	HLA-C*12:03	155
	73-48	WIIMGLNKIVRMYSPTSI	153	RMYSPTSI	HLA-C*12:03	21
				VRMYSPTSI	HLA-C*07:01	87
				WIIMGLNKI	HLA-C*12:03	163
				IIMGLNKI	HLA-C*12:03	187
				WIIMGLNKIV	HLA-C*12:03	256

Table 1 Continued

participant	ID	18mer AA sequence	DC1-stimulated IFN-g SFC/10^6	MHC-1 restricted epitope AA sequence	Class 1 restriction	ic50
				IIMGLNKIV	HLA-C*12:03	312
				WIIMGLNKIVRMY	HLA-A*25:01	314
				WIIMGLNKIVRMY	HLA-C*12:03	367
				IIMGLNKIVRMY	HLA-C*12:03	484
				IVRMYSPTSI	HLA-C*12:03	506
	73-54	PKEPFRDYVDRFYKTLRA	141	YVDRFYKTL	HLA-C*12:03	8
				EPFRDYVDRFYKTL	HLA-C*12:03	75
				FRDYVDRFYKTL	HLA-C*07:01	298
				DYVDRFYKTL	HLA-C*12:03	313
				YVDRFYKTLRA	HLA-A*01:01	405
	73-55	FRDYVDRFYKTLRAEQAS	231	YVDRFYKTL	HLA-C*12:03	8
				FRDYVDRFYKTL	HLA-C*07:01	298
				DYVDRFYKTL	HLA-C*12:03	313
				YVDRFYKTLRA	HLA-A*01:01	405
	73-57	YKTLRAEQASQEVKNWMT	7641	AEQASQEVKNW	HLA-B*44:03	19
				LRAEQASQEV	HLA-C*07:01	21
				RAEQASQEV	HLA-C*12:03	79
				LRAEQASQEVKNWM	HLA-C*07:01	179
				AEQASQEVKNWM	HLA-B*44:03	401
				YKTLRAEQASQEV	HLA-C*07:01	491
	73-58	RAEQASQEVKNWMTETLL	6881	AEQASQEVKNW	HLA-B*44:03	19
				QASQEVKNWMTETL	HLA-C*12:03	61
				RAEQASQEV	HLA-C*12:03	79
				EVKNWMTETL	HLA-C*12:03	361
				AEQASQEVKNWM	HLA-B*44:03	401
	73-59	ASQEVKNWMTETLLVQNS	631	WMTETLLV	HLA-C*12:03	255
				EVKNWMTETL	HLA-C*12:03	361
				QEVKNWMTETLLVQ	HLA-B*18:01	483
				EVKNWMTETLLV	HLA-C*12:03	495
				QEVKNWMTETLLV	HLA-B*44:03	502
	73-60	VKNWMTETLLVQNSNPDC	211	WMTETLLV	HLA-C*12:03	255
	73-61	MTETLLVQNSNPDCKTIL	561	NSNPDCKTI	HLA-C*12:03	23
				VQNSNPDCKTI	HLA-C*12:03	103
				LLVQNSNPDCKTI	HLA-C*12:03	183
				NSNPDCKTIL	HLA-C*12:03	184
				LVQNSNPDCKTI	HLA-C*12:03	189
				SNPDCKTIL	HLA-C*07:01	395
	73-63A	NSNPDCKTILKALGPGAT	401	NSNPDCKTI	HLA-C*12:03	23
				NSNPDCKTIL	HLA-C*12:03	184
				NSNPDCKTILKAL	HLA-C*12:03	370
				SNPDCKTIL	HLA-C*07:01	395
	73-67	ATLEEMMTACQGVGGPGH	231	EEMMTACQGV	HLA-B*44:03	317

From left to right: 1. Study participant identification number. 2. Name of 18-mers containing predicted autologous variants of MHC class I-restricted epitopes. 3. The amino acid (AA) sequences of 18-mers. 4. The mean IFN-γ response detected in DC-stimulated memory T cells is shown as the number of IFN-γ-producing spot-forming cells per 10^6 responders (IFN-γ SFC/10^6). 5. MHC class I-restriction for each participant's HLA alleles. 6. IC50nM value

for each predicted MHC class I-restricted HIV-1 *gag* epitopes. The predicted output from the algorithm is given in units of IC50nM. A lower number indicates higher affinity.

Table 2. The predicted MHC class I-restricted epitopes for participant S5

participant	ID	18mer AA sequence	DC1-stimulated IFN-g SFC/10^6	MHC-1 restricted epitope AA sequence	Class 1 restriction	ic50
S5	71-12	QTGSEELKSLYNTVATLY	5607	SLYNTVATLY	HLA-B*15:01	14.67
				SLYNTVATL	HLA-A*02:01	53.76
				SLYNTVATL	HLA-B*15:01	123.55
				KSLYNTVATL	HLA-B*15:01	193.81
				KSLYNTVATL	HLA-A*02:01	196.03
				SLYNTVATL	HLA-C*03:03	242.76
				SEELKSLY	HLA-B*44:02	366.03
	71-13	EELKSLYNTVATLYCVHQ	3525	SLYNTVATLY	HLA-B*15:01	14.67
				SLYNTVATL	HLA-A*02:01	53.76
				SLYNTVATLYCV	HLA-A*02:01	92.08
				SLYNTVATL	HLA-B*15:01	123.55
				KSLYNTVATLYCV	HLA-A*02:01	137.95
				LKSLYNTVATLYCV	HLA-A*02:01	174.61
				YNTVATLYCV	HLA-A*02:01	178.91
				KSLYNTVATL	HLA-B*15:01	193.81
				KSLYNTVATL	HLA-A*02:01	196.03
				SLYNTVATL	HLA-C*03:03	242.76
				SLYNTVATLYCVH	HLA-A*02:01	391.83
				NTVATLYCV	HLA-A*02:01	444.9
	71-14	SLYNTVATLYCVHQRIEV	11087	SLYNTVATLY	HLA-B*15:01	14.67
				SLYNTVATL	HLA-A*02:01	53.76
				SLYNTVATLYCV	HLA-A*02:01	92.08
				SLYNTVATL	HLA-B*15:01	123.55
				YCVHQRIEV	HLA-C*03:03	163.79
				YNTVATLYCV	HLA-A*02:01	178.91
				SLYNTVATL	HLA-C*03:03	242.76
				TLYCVHQRI	HLA-A*02:01	256.91
				TLYCVHQRIEV	HLA-A*02:01	286.98
				SLYNTVATLYCVH	HLA-A*02:01	391.83
				NTVATLYCV	HLA-A*02:01	444.9
				ATLYCVHQRIEV	HLA-A*02:01	453.09
	71-23	EKAFSPEVIPMFSALSEG	3251	EVIPMFSAL	HLA-A*26:02	6.88
				EVIPMFSAL	HLA-C*03:03	48.57
				FSPEVIPMF	HLA-A*26:02	65.9
				KAFSPEVIPM	HLA-B*15:01	268.88
				FSPEVIPMF	HLA-C*05:01	274.36
				AFSPEVIPM	HLA-C*03:03	380.94
	71-24	SPEVIPMFSALSEGATPQ	13580	EVIPMFSAL	HLA-A*26:02	6.88
				EVIPMFSAL	HLA-C*03:03	48.57
	71-35	AAEWDRLHPVHAGPIAPG	1553	AAEWDRLHPV	HLA-A*02:01	259.74
				RLHPVHAGPI	HLA-B*15:01	266.88
				AEWDRLHPV	HLA-B*44:02	311.79
	71-47	IYKRWIILGLNKIVRMYS	4813	LGLNKIVRMY	HLA-B*15:01	209.81
				GLNKIVRMY	HLA-B*15:01	381.8
				ILGLNKIVRM	HLA-A*02:01	496.96
	71-48	WIILGLNKIVRMYSPSSI	6457	LGLNKIVRMY	HLA-B*15:01	209.81
				GLNKIVRMY	HLA-B*15:01	381.8
				ILGLNKIVRM	HLA-A*02:01	496.96
	71-49	GLNKIVRMYSPSSILDIK	11607	RMYSPSSIL	HLA-C*03:03	7.14
				RMYSPSSIL	HLA-B*15:01	45.85
				VRMYSPSSIL	HLA-B*15:01	232.73
				RMYSPSSIL	HLA-A*02:01	375.04
				GLNKIVRMY	HLA-B*15:01	381.8
	73-57	YKTLRAEQASQEVKNWMT	6292	AEQASQEVKNW	HLA-B*44:02	40.98
				RAEQASQEV	HLA-C*03:03	85.91
				AEQASQEVKNWM	HLA-B*44:02	90.37
				RAEQASQEVKNW	HLA-B*44:02	106

Table 2 Continued

participant	ID	18mer AA sequence	DC1-stimulated IFN-g SFC/10^6	MHC-1 restricted epitope AA sequence	Class 1 restriction	ic50
				AEQASQEVKNWMT	HLA-B*44:02	130.74
				LRAEQASQEVKNW	HLA-B*44:02	160.05
				TLRAEQASQEVKNW	HLA-B*44:02	189.36
				RAEQASQEVKNWM	HLA-B*44:02	258.28
				RAEQASQEVKNWMT	HLA-B*44:02	379.25
				LRAEQASQEVKNWM	HLA-B*44:02	395.47
	71-58	RAEQASQEVKNWMTETLL	5689	AEQASQEVKNW	HLA-B*44:02	40.98
				RAEQASQEV	HLA-C*03:03	85.91
				AEQASQEVKNWM	HLA-B*44:02	90.37
				RAEQASQEVKNW	HLA-B*44:02	106
				AEQASQEVKNWMT	HLA-B*44:02	130.74
				AEQASQEVKNWMTE	HLA-B*44:02	151.33
				EVKNWMTET	HLA-A*26:02	157.5
				RAEQASQEVKNWM	HLA-B*44:02	258.28
				RAEQASQEVKNWMT	HLA-B*44:02	379.25
	73-64A	DCKTILKALGPGATLEEM	3443	KALGPGATL	HLA-C*03:03	2.83
				ALGPGATL	HLA-C*03:03	64.52
				LKALGPGATL	HLA-C*03:03	182.12
				KALGPGATLE	HLA-C*03:03	203.23
				LKALGPGATLE	HLA-C*03:03	363.48
				KALGPGATLEE	HLA-C*03:03	374.83
				KALGPGATLEEM	HLA-C*03:03	386.02
				ILKALGPGATL	HLA-C*03:03	394.95
				LKALGPGATLEE	HLA-C*03:03	396.94
				LKALGPGATLEEM	HLA-C*03:03	408.79
				TILKALGPGATL	HLA-C*03:03	424.95
				KTILKALGPGATL	HLA-C*03:03	459.62
				CKTILKALGPGATL	HLA-C*03:03	472.74
				ILKALGPGATLE	HLA-C*03:03	487.14
	71-65	ILKALGPAATLEEMMTAC	2374	KALGPAATL	HLA-C*03:03	3.38
				ALGPAATL	HLA-C*03:03	126.86
				ATLEEMMTA	HLA-A*02:01	330.9
				LKALGPAATL	HLA-C*03:03	360.19
				KALGPAATLE	HLA-C*03:03	394.96
	71-70	VGGPGHKARVLAEAMSQV	10511	VLAEAMSQV	HLA-A*02:01	9.73
				RVLAEAMSQV	HLA-A*02:01	99.25

From left to right: 1. Study participant identification number. 2. Name of 18-mers containing predicted autologous variants of MHC class I-restricted epitopes. 3. The amino acid (AA) sequences of 18-mers. 4. The mean IFN-γ response detected in DC-stimulated memory T cells is shown as the number of IFN-γ-producing spot-forming cells per 10^6 responders (IFN-γ SFC/10^6). 5. MHC class I-restriction for each participant's HLA alleles. 6. IC50nM value for each predicted MHC class I-restricted HIV-1 *gag* epitopes. The predicted output from the algorithm is given in units of IC50nM. A lower number indicates higher affinity

4.5 VIRAL MUTATION WAS IDENTIFIED THROUGH GAG SEQUENCE ALIGNMENT BY YEAR

To study the viral evolution, it is also important to know course of disease. For S4, the patient had seroconversion in 07/21/1987 and received cART treatment at 02/21/1996. S5 had seroconversion in 03/24/1987 and received cART treatment since 11/20/2002.

The course of disease for both S4 and S5 (Fig.10) indicates a good efficacy of cART with a significant recovery of $CD4^+$ T cell counting and low viral load.

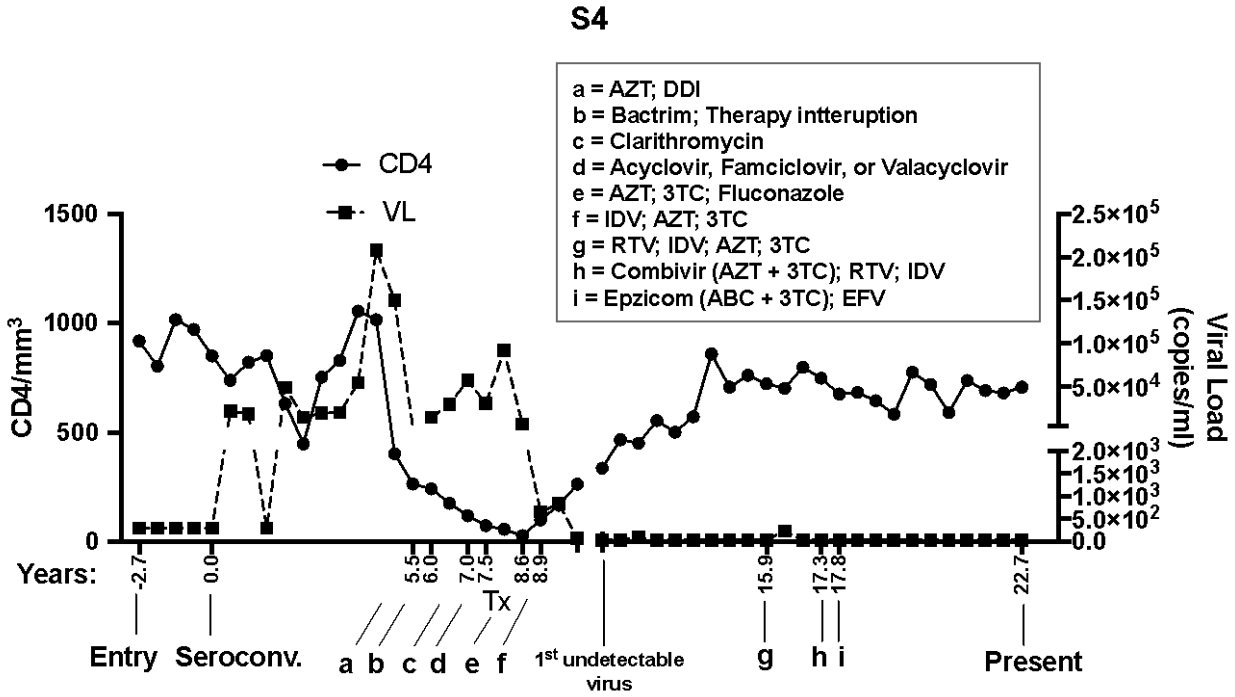

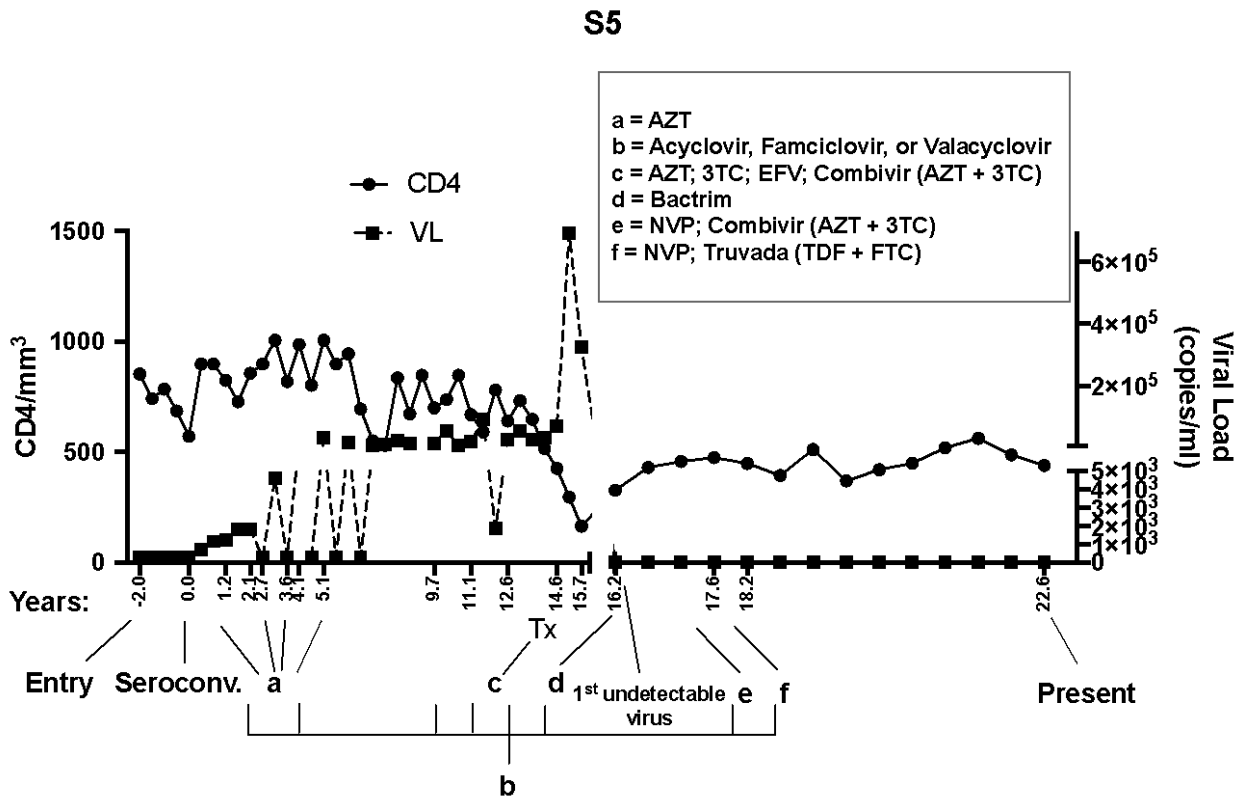

Figure 10. Participants' clinical history with CD4⁺ T cell counts, medication and viral load history

The HIV-1 viral load (square symbols, dashed line) is expressed as copies/ml. The $CD4^+$ T cell counts (round symbols, continuous line) are expressed as absolute number/ mm^3. Study entry, initiation of therapy (cART) are expressed in years. The estimated time of seroconversion is taken as the time 0 value. AZT: Retrovir (zidovudine); DDI: Didanosine; 3TC: Lamivudine; IDV: Indinavir; RTV: Ritonavir; ABC: Abacavir; EFV: Efavirenz; NVP: Nevirapine; TDF: Tenofovir.

In order to locate mutation region, I then aligned whole *gag* sequences by year (Fig. 11 and Fig.12). I have access to the S4 viral *gag* p17 and p24 sequences of year 1987, 1988, 1989, 1991, 1992, 1993, 1996 and 2013, which is year 0, 1, 2, 4, 5, 6, 9, and 26 post seroconversion (Fig.11). The 2013 sequence is shown as "consensus" which was assembled from 20 clones and as "subdominant" which represents clones where a mutation was present less than 5 but more than 3

times. For S5, I have viral *gag* p17 and p24 sequences of year 1987, 1990, 1993, 1997, 2000, 2001, 2002, 2013, which is year 0, 3, 6, 10, 13, 14, 15, and 26 post seroconversion (Fig.12).

To get a better idea of the value of each “hot spot” and make some considerations on the impact of mutations on CTL, IFN-γ ELISpot results were also ranked in four groups: group #1 number of responses between 1 and 10%, group #2 number of responses between 11and 25%, group #3 number of responses between 26 and 50%, group #4 number of responses between 51and 100% as t shown in the figure.

Having aligned the viral sequence by year, the viral mutations were identified. In general, for both S4 and S5 *gag* sequences, there are relatively few mutations throughout the years. Of a total of 13 mutations in S4 *gag* only 2 are in regions not recognized by memory CTLs. All the 13 mutations in S5 *gag* can be recognized by memory CTLs.

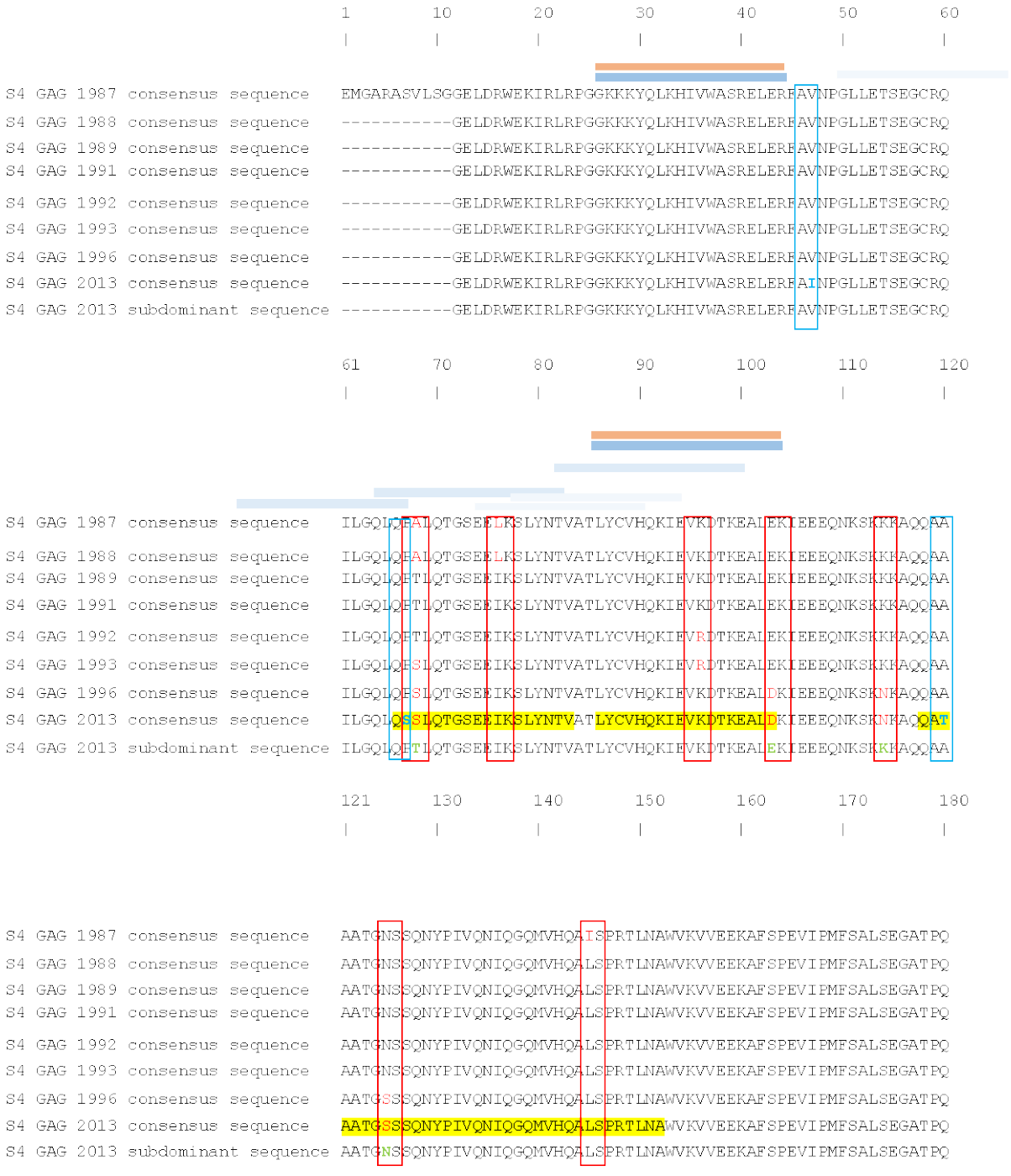
1 10 20 30 40 50 60
S4 GAG 1987 consensus sequence EMGARASVLSGGELDRWEKIRLRPGGKKKYQLKHIVWASRELERFAVNPGLLETSEGCRQ
S4 GAG 1988 consensus sequence ----------GELDRWEKIRLRPGGKKKYQLKHIVWASRELERFAVNPGLLETSEGCRQ
S4 GAG 1989 consensus sequence ----------GELDRWEKIRLRPGGKKKYQLKHIVWASRELERFAVNPGLLETSEGCRQ
S4 GAG 1991 consensus sequence ----------GELDRWEKIRLRPGGKKKYQLKHIVWASRELERFAVNPGLLETSEGCRQ
S4 GAG 1992 consensus sequence ----------GELDRWEKIRLRPGGKKKYQLKHIVWASRELERFAVNPGLLETSEGCRQ
S4 GAG 1993 consensus sequence ----------GELDRWEKIRLRPGGKKKYQLKHIVWASRELERFAVNPGLLETSEGCRQ
S4 GAG 1996 consensus sequence ----------GELDRWEKIRLRPGGKKKYQLKHIVWASRELERFAVNPGLLETSEGCRQ
S4 GAG 2013 consensus sequence ----------GELDRWEKIRLRPGGKKKYQLKHIVWASRELERFAINPGLLETSEGCRQ
S4 GAG 2013 subdominant sequence ----------GELDRWEKIRLRPGGKKKYQLKHIVWASRELERFAVNPGLLETSEGCRQ
61 70 80 90 100 110 120
S4 GAG 1987 consensus sequence ILGQLQPALQTGSEELKSLYNTVATLYCVHQKIEVKDTKEALEKIEEEQNKSKKKAQQAA
S4 GAG 1988 consensus sequence ILGQLQPALQTGSEELKSLYNTVATLYCVHQKIEVKDTKEALEKIEEEQNKSKKKAQQAA
S4 GAG 1989 consensus sequence ILGQLQPTLQTGSEEIKSLYNTVATLYCVHQKIEVKDTKEALEKIEEEQNKSKKKAQQAA
S4 GAG 1991 consensus sequence ILGQLQPTLQTGSEEIKSLYNTVATLYCVHQKIEVKDTKEALEKIEEEQNKSKKKAQQAA
S4 GAG 1992 consensus sequence ILGQLQPTLQTGSEEIKSLYNTVATLYCVHQKIEVRDTKEALEKIEEEQNKSKKKAQQAA
S4 GAG 1993 consensus sequence ILGQLQPSLQTGSEEIKSLYNTVATLYCVHQKIEVRDTKEALEKIEEEQNKSKKKAQQAA
S4 GAG 1996 consensus sequence ILGQLQPSLQTGSEEIKSLYNTVATLYCVHQKIEVKDTKEALDKIEEEQNKSKNKAQQAA
S4 GAG 2013 consensus sequence ILGQLQSSLQTGSEEIKSLYNTVATLYCVHQKIEVKDTKEALDKIEEEQNKSKNKAQQAT
S4 GAG 2013 subdominant sequence ILGQLQPTLQTGSEEIKSLYNTVATLYCVHQKIEVKDTKEALEKIEEEQNKSKKKAQQAA
121 130 140 150 160 170 180
S4 GAG 1987 consensus sequence AATGNSSQNYPIVQNIQGQMVHQAISPRTLNAWVKVVEEKAFSPEVIPMFSALSEGATPQ
S4 GAG 1988 consensus sequence AATGNSSQNYPIVQNIQGQMVHQALSPRTLNAWVKVVEEKAFSPEVIPMFSALSEGATPQ
S4 GAG 1989 consensus sequence AATGNSSQNYPIVQNIQGQMVHQALSPRTLNAWVKVVEEKAFSPEVIPMFSALSEGATPQ
S4 GAG 1991 consensus sequence AATGNSSQNYPIVQNIQGQMVHQALSPRTLNAWVKVVEEKAFSPEVIPMFSALSEGATPQ
S4 GAG 1992 consensus sequence AATGNSSQNYPIVQNIQGQMVHQALSPRTLNAWVKVVEEKAFSPEVIPMFSALSEGATPQ
S4 GAG 1993 consensus sequence AATGNSSQNYPIVQNIQGQMVHQALSPRTLNAWVKVVEEKAFSPEVIPMFSALSEGATPQ
S4 GAG 1996 consensus sequence AATGSSSQNYPIVQNIQGQMVHQALSPRTLNAWVKVVEEKAFSPEVIPMFSALSEGATPQ
S4 GAG 2013 consensus sequence AATGSSSQNYPIVQNIQGQMVHQALSPRTLNAWVKVVEEKAFSPEVIPMFSALSEGATPQ
S4 GAG 2013 subdominant sequence AATGNSSQNYPIVQNIQGQMVHQALSPRTLNAWVKVVEEKAFSPEVIPMFSALSEGATPQ

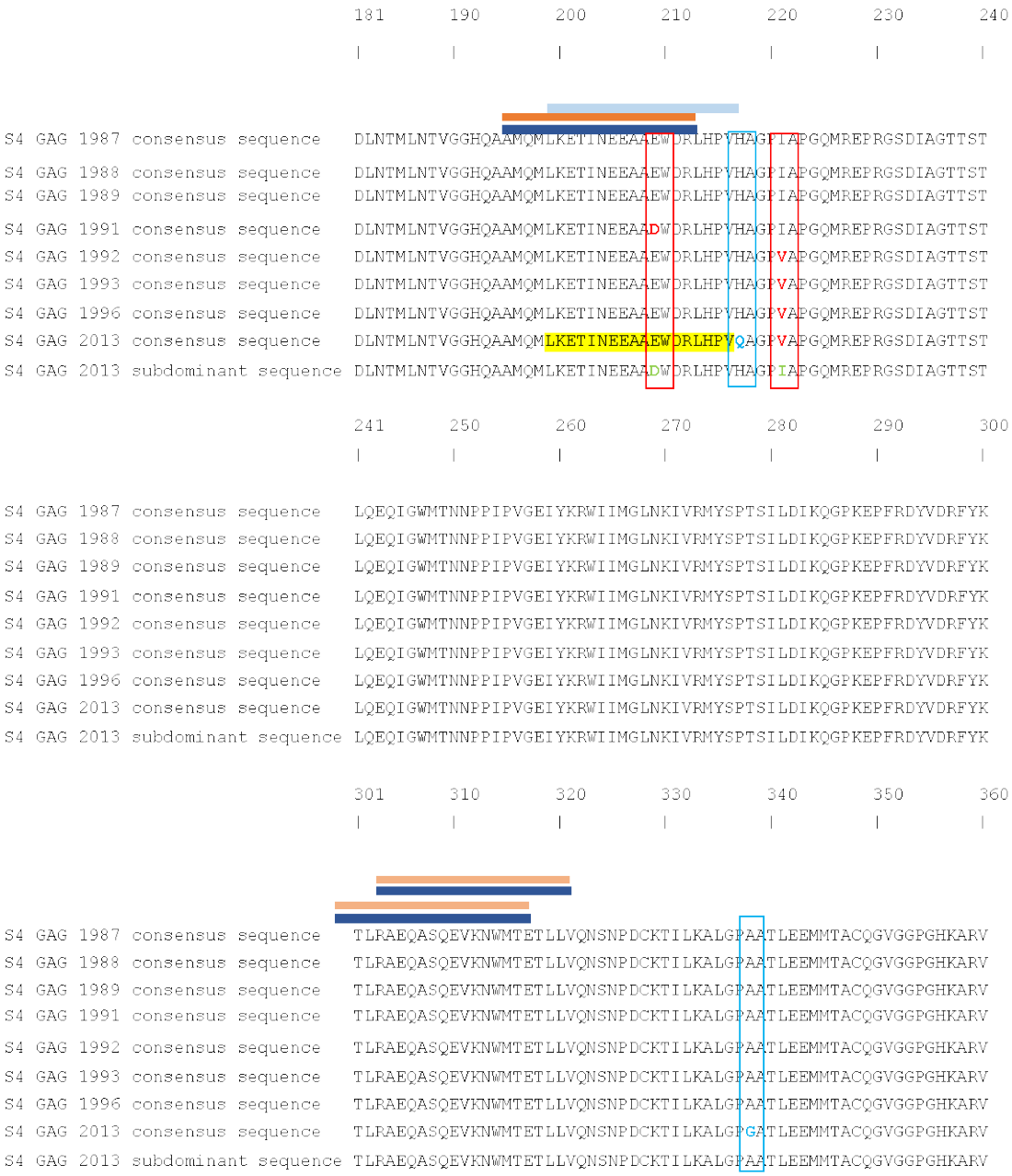
181 190 200 210 220 230 240
S4 GAG 1987 consensus sequence DLNTMLNTVGGHQAAMQMLKETINEEAAEWDRLHPVHAGPIAPGQMREPRGSDIAGTTST
S4 GAG 1988 consensus sequence DLNTMLNTVGGHQAAMQMLKETINEEAAEWDRLHPVHAGPIAPGQMREPRGSDIAGTTST
S4 GAG 1989 consensus sequence DLNTMLNTVGGHQAAMQMLKETINEEAAEWDRLHPVHAGPIAPGQMREPRGSDIAGTTST
S4 GAG 1991 consensus sequence DLNTMLNTVGGHQAAMQMLKETINEEAADWDRLHPVHAGPIAPGQMREPRGSDIAGTTST
S4 GAG 1992 consensus sequence DLNTMLNTVGGHQAAMQMLKETINEEAAEWDRLHPVHAGPVAPGQMREPRGSDIAGTTST
S4 GAG 1993 consensus sequence DLNTMLNTVGGHQAAMQMLKETINEEAAEWDRLHPVHAGPVAPGQMREPRGSDIAGTTST
S4 GAG 1996 consensus sequence DLNTMLNTVGGHQAAMQMLKETINEEAAEWDRLHPVHAGPVAPGQMREPRGSDIAGTTST
S4 GAG 2013 consensus sequence DLNTMLNTVGGHQAAMQMLKETINEEAAEWDRLHPVQAGPVAPGQMREPRGSDIAGTTST
S4 GAG 2013 subdominant sequence DLNTMLNTVGGHQAAMQMLKETINEEAADWDRLHPVHAGPIAPGQMREPRGSDIAGTTST
241 250 260 270 280 290 300
S4 GAG 1987 consensus sequence LQEQIGWMTNNPPIPVGEIYKRWIIMGLNKIVRMYSPTSILDIKQGPKEPFRDYVDRFYK
S4 GAG 1988 consensus sequence LQEQIGWMTNNPPIPVGEIYKRWIIMGLNKIVRMYSPTSILDIKQGPKEPFRDYVDRFYK
S4 GAG 1989 consensus sequence LQEQIGWMTNNPPIPVGEIYKRWIIMGLNKIVRMYSPTSILDIKQGPKEPFRDYVDRFYK
S4 GAG 1991 consensus sequence LQEQIGWMTNNPPIPVGEIYKRWIIMGLNKIVRMYSPTSILDIKQGPKEPFRDYVDRFYK
S4 GAG 1992 consensus sequence LQEQIGWMTNNPPIPVGEIYKRWIIMGLNKIVRMYSPTSILDIKQGPKEPFRDYVDRFYK
S4 GAG 1993 consensus sequence LQEQIGWMTNNPPIPVGEIYKRWIIMGLNKIVRMYSPTSILDIKQGPKEPFRDYVDRFYK
S4 GAG 1996 consensus sequence LQEQIGWMTNNPPIPVGEIYKRWIIMGLNKIVRMYSPTSILDIKQGPKEPFRDYVDRFYK
S4 GAG 2013 consensus sequence LQEQIGWMTNNPPIPVGEIYKRWIIMGLNKIVRMYSPTSILDIKQGPKEPFRDYVDRFYK
S4 GAG 2013 subdominant sequence LQEQIGWMTNNPPIPVGEIYKRWIIMGLNKIVRMYSPTSILDIKQGPKEPFRDYVDRFYK
301 310 320 330 340 350 360
S4 GAG 1987 consensus sequence TLRAEQASQEVKNWMTETLLVQNSNPDCKTILKALGPAATLEEMMTACQGVGGPGHKARV
S4 GAG 1988 consensus sequence TLRAEQASQEVKNWMTETLLVQNSNPDCKTILKALGPAATLEEMMTACQGVGGPGHKARV
S4 GAG 1989 consensus sequence TLRAEQASQEVKNWMTETLLVQNSNPDCKTILKALGPAATLEEMMTACQGVGGPGHKARV
S4 GAG 1991 consensus sequence TLRAEQASQEVKNWMTETLLVQNSNPDCKTILKALGPAATLEEMMTACQGVGGPGHKARV
S4 GAG 1992 consensus sequence TLRAEQASQEVKNWMTETLLVQNSNPDCKTILKALGPAATLEEMMTACQGVGGPGHKARV
S4 GAG 1993 consensus sequence TLRAEQASQEVKNWMTETLLVQNSNPDCKTILKALGPAATLEEMMTACQGVGGPGHKARV
S4 GAG 1996 consensus sequence TLRAEQASQEVKNWMTETLLVQNSNPDCKTILKALGPAATLEEMMTACQGVGGPGHKARV
S4 GAG 2013 consensus sequence TLRAEQASQEVKNWMTETLLVQNSNPDCKTILKALGPGATLEEMMTACQGVGGPGHKARV
S4 GAG 2013 subdominant sequence TLRAEQASQEVKNWMTETLLVQNSNPDCKTILKALGPAATLEEMMTACQGVGGPGHKARV

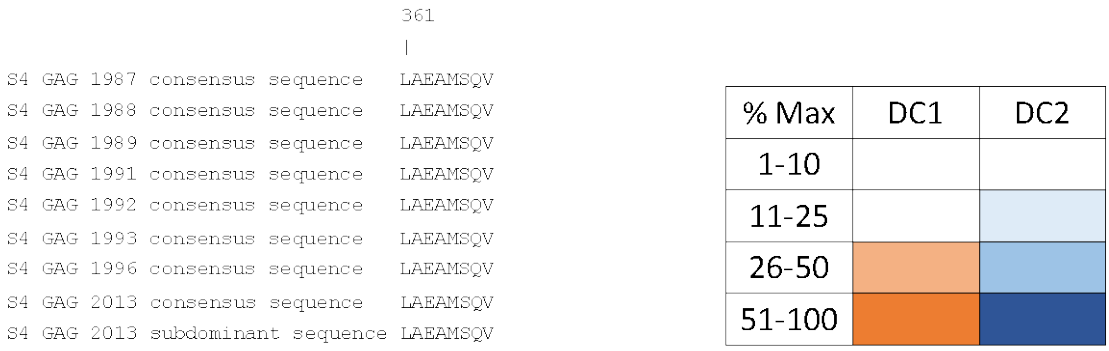

Figure 11. S4 aligned *gag* p17&p24 sequence by year

S4 *gag* p17 and p24 sequence aligned by years. On top of each sequence alignment, the bars covering the length of 18 amino acids and color coded according to the legend below. The red character shows where the mutation has been occurred and the blue ones are new mutations in 2015. The five candidate 18-mer peptides are highlighted in yellow.

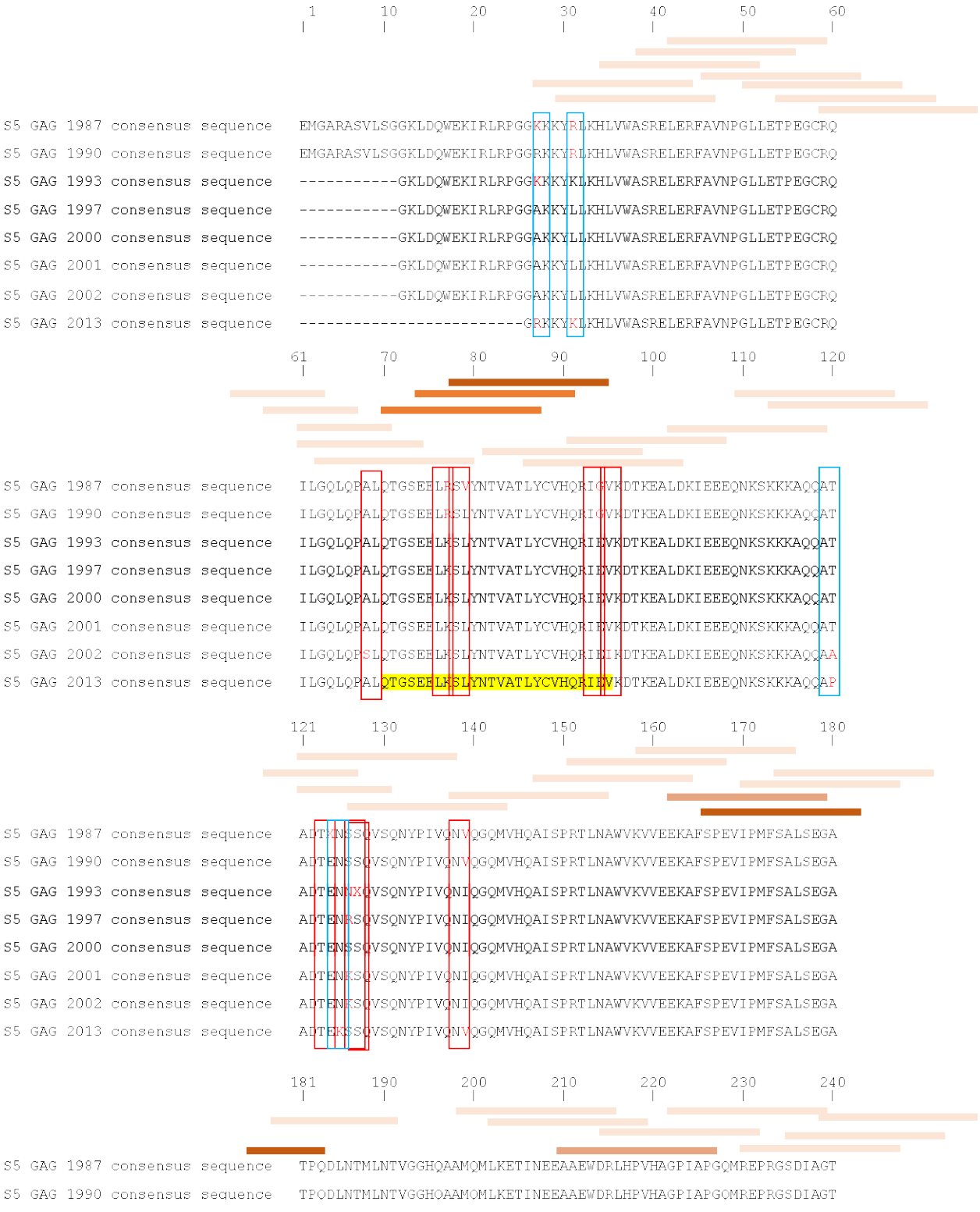
1 10 20 30 40 50 60
S5 GAG 1987 consensus sequence EMGARASVLSGGKLDQWEKIRLRPGGKKKYRLKHLVWASRELERFAVNPGLLETPEGCRQ
S5 GAG 1990 consensus sequence EMGARASVLSGGKLDQWEKIRLRPGGRKKYRLKHLVWASRELERFAVNPGLLETPEGCRQ
S5 GAG 1993 consensus sequence ----------GKLDQWEKIRLRPGGKKKYKLKHLVWASRELERFAVNPGLLETPEGCRQ
S5 GAG 1997 consensus sequence ----------GKLDQWEKIRLRPGGAKKYLLKHLVWASRELERFAVNPGLLETPEGCRQ
S5 GAG 2000 consensus sequence ----------GKLDQWEKIRLRPGGAKKYLLKHLVWASRELERFAVNPGLLETPEGCRQ
S5 GAG 2001 consensus sequence ----------GKLDQWEKIRLRPGGAKKYLLKHLVWASRELERFAVNPGLLETPEGCRQ
S5 GAG 2002 consensus sequence ----------GKLDQWEKIRLRPGGAKKYLLKHLVWASRELERFAVNPGLLETPEGCRQ
S5 GAG 2013 consensus sequence ----------GRKKYKLKHLVWASRELERFAVNPGLLETPEGCRQ
61 70 80 90 100 110 120
S5 GAG 1987 consensus sequence ILGQLQPALQTGSEELRSVYNTVATLYCVHQRIGVKDTKEALDKIEEEQNKSKKKAQQAT
S5 GAG 1990 consensus sequence ILGQLQPALQTGSEELRSLYNTVATLYCVHQRIGVKDTKEALDKIEEEQNKSKKKAQQAT
S5 GAG 1993 consensus sequence ILGQLQPALQTGSEELKSLYNTVATLYCVHQRIEVKDTKEALDKIEEEQNKSKKKAQQAT
S5 GAG 1997 consensus sequence ILGQLQPALQTGSEELKSLYNTVATLYCVHQRIEVKDTKEALDKIEEEQNKSKKKAQQAT
S5 GAG 2000 consensus sequence ILGQLQPALQTGSEELKSLYNTVATLYCVHQRIEVKDTKEALDKIEEEQNKSKKKAQQAT
S5 GAG 2001 consensus sequence ILGQLQPALQTGSEELKSLYNTVATLYCVHQRIEVKDTKEALDKIEEEQNKSKKKAQQAT
S5 GAG 2002 consensus sequence ILGQLQPSLQTGSEELKSLYNTVATLYCVHQRIEIKDTKEALDKIEEEQNKSKKKAQQAA
S5 GAG 2013 consensus sequence ILGQLQPALQTGSEELKSLYNTVATLYCVHQRIEVKDTKEALDKIEEEQNKSKKKAQQAP
121 130 140 150 160 170 180
S5 GAG 1987 consensus sequence ADTKNSSQVSQNYPIVQNVQGQMVHQAISPRTLNAWVKVVEEKAFSPEVIPMFSALSEGA
S5 GAG 1990 consensus sequence ADTENSSQVSQNYPIVQNVQGQMVHQAISPRTLNAWVKVVEEKAFSPEVIPMFSALSEGA
S5 GAG 1993 consensus sequence ADTENMXQVSQNYPIVQNIQGQMVHQAISPRTLNAWVKVVEEKAFSPEVIPMFSALSEGA
S5 GAG 1997 consensus sequence ADTENRSQVSQNYPIVQNIQGQMVHQAISPRTLNAWVKVVEEKAFSPEVIPMFSALSEGA
S5 GAG 2000 consensus sequence ADTENSSQVSQNYPIVQNIQGQMVHQAISPRTLNAWVKVVEEKAFSPEVIPMFSALSEGA
S5 GAG 2001 consensus sequence ADTENKSQVSQNYPIVQNIQGQMVHQAISPRTLNAWVKVVEEKAFSPEVIPMFSALSEGA
S5 GAG 2002 consensus sequence ADTENKSQVSQNYPIVQNIQGQMVHQAISPRTLNAWVKVVEEKAFSPEVIPMFSALSEGA
S5 GAG 2013 consensus sequence ADTEKSSQVSQNYPIVQNVQGQMVHQAISPRTLNAWVKVVEEKAFSPEVIPMFSALSEGA
181 190 200 210 220 230 240
S5 GAG 1987 consensus sequence TPQDLNTMLNTVGGHQAAMQMLKETINEEAAEWDRLHPVHAGPIAPGQMREPRGSDIAGT
S5 GAG 1990 consensus sequence TPQDLNTMLNTVGGHQAAMQMLKETINEEAAEWDRLHPVHAGPIAPGQMREPRGSDIAGT

S5 GAG 1993 consensus sequence TPQDLNTMLNTVGGHQAAMQMLKETINEEAAEWDRLHPVHAGPIAPGQMREPRGSDIAGT
S5 GAG 1997 consensus sequence TPQDLNTMLNTVGGHQAAMQMLKETINEEAAEWDRLHPVHAGPIAPGQMREPRGSDIAGT
S5 GAG 2000 consensus sequence TPQDLNTMLNTVGGHQAAMQMLKETINEEAAEWDRLHPVHAGPIAPGQMREPRGSDIAGT
S5 GAG 2001 consensus sequence TPQDLNTMLNTVGGHQAAMQMLKETINEEAAEWDRLHPVHAGPIAPGQMREPRGSDIAGT
S5 GAG 2002 consensus sequence TPQDLNTMLNTVGGHQAAMQMLKETINEEAAEWDRLHPVHAGPIAPGQMREPRGSDIAGT
S5 GAG 2013 consensus sequence TPQDLNTMLNTVGGHQAAMQMLKETINEEAAEWDRLHPVHAGPIAPGQMREPRGSDIAGT

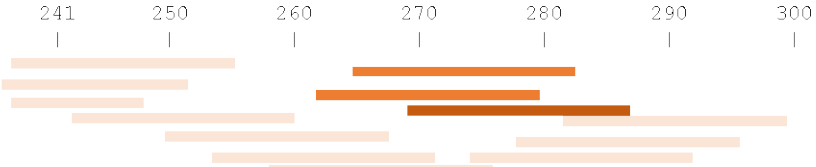

S5 GAG 1987 consensus sequence TSTLQEQIGWMTHNPPIPVGEIYKRWIILGLNKIVRMYSPSSILDIKQGPKEPFRDYVDR
S5 GAG 1990 consensus sequence TSTLQEQIGWMTHNPPIPVGEIYKRWIILGLNKIVRMYSPSSILDIKQGPKEPFRDYVDR
S5 GAG 1993 consensus sequence TSTLQEQIGWMTHNPPIPVGEIYKRWIILGLNKIVRMYSPSSILDIKQGPKEPFRDYVDR
S5 GAG 1997 consensus sequence TSTLQEQIGWMTHNPPIPVGEIYKRWIILGLNKIVRMYSPSSILDIKQGPKEPFRDYVDR
S5 GAG 2000 consensus sequence TSTLQEQIGWMTHNPPIPVGEIYKRWIILGLNKIVRMYSPSSILDIKQGPKEPFRDYVDR
S5 GAG 2001 consensus sequence TSTLQEQIGWMTHNPPIPVGEIYKRWIILGLNKIVRMYSPSSILDIKQGPKEPFRDYVDR
S5 GAG 2002 consensus sequence TSTLQEQIGWMTHNPPIPVGEIYKRWIILGLNKIVRMYSPSSILDIKQGPKEPFRDYVDR
S5 GAG 2013 consensus sequence TSTLQEQIGWMTHNPPIPVGEIYKRWIILGLNKIVRMYSPSSILDIKQGPKEPFRDYVDR

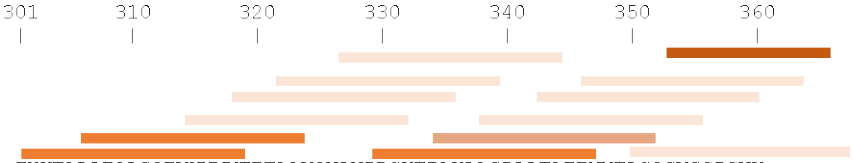

S5 GAG 1987 consensus sequence FYKTLRAEQASQEVKNWMTETLLVQNANPDCKTILKALGPAATLEEMMTACQGVGGPGHK
S5 GAG 1990 consensus sequence FYKTLRAEQASQEVKNWMTETLLVQNANPDCKTILKALGPAATLEEMMTACQGVGGPGHK
S5 GAG 1993 consensus sequence FYKTLRAEQASQEVKNWMTETLLVQNANPDCKTILKALGPAATLEEMMTACQGVGGPGHK
S5 GAG 1997 consensus sequence FYKTLRAEQASQEVKNWMTETLLVQNANPDCKTILKALGPAATLEEMMTACQGVGGPGHK
S5 GAG 2000 consensus sequence FYKTLRAEQASQEVKNWMTETLLVQNANPDCKTILKALGPAATLEEMMTACQGVGGPGHK
S5 GAG 2001 consensus sequence FYKTLRAEQASQEVKNWMTETLLVQNANPDCKTILKALGPAATLEEMMTACQGVGGPGHK
S5 GAG 2002 consensus sequence FYKTLRAEQASQEVKNWMTETLLVQNANPDCKTILKALGPAATLEEMMTACQGVGGPGHK
S5 GAG 2013 consensus sequence FYKTLRAEQASQEVKNWMTETLLVQNANPDCKTILKALGPAATLEEMMTACQGVGGPGHK

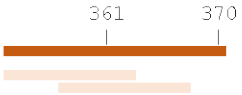

S5 GAG 1987 consensus sequence ARVLAEAMSQVTNSA
S5 GAG 1990 consensus sequence ARVLAEAMSQVTNSA
S5 GAG 1993 consensus sequence ARVLAEAMSQVTNSA
S5 GAG 1997 consensus sequence ARVLAEAMSQVTNSA
S5 GAG 2000 consensus sequence ARVLAEAMSQVTNSA
S5 GAG 2001 consensus sequence ARVLAEAMSQVTNSA
S5 GAG 2002 consensus sequence ARVLAEAMSQVTNSA
S5 GAG 2013 consensus sequence ARVLAEAMSQVTNSA

%max	αDC1
1-10	
11-25	
26-50	
50-100	

Figure 12. S5 aligned *gag* p17&p24 sequence by year

S5 *gag* p17 and p24 sequence aligned by years. On top of each sequence alignment, the bars covering the length of 18 amino acids and color coded according to the legend below. The red character shows where the mutation has been occurred and the blue ones are new mutations in 2013. The three candidate 18-mer peptides are highlighted in yellow.

4.6 PRELIMINARY COMPARISON OF MEMORY CTL RESPONSE AGAINST FOUNDER EPITOPES VERSUS RESERVOIR EPITOPES USING MHC-1 BINDING PREDICTIVE ALGORITHM

To focus on the viral mutation, I then ruled out all the predicted potential epitopes without mutation. Five 18-mers were identified for S4 and three for S5 (Table 3). After excluded all the identical epitopes, for S4, I got 15 candidate epitopes corresponding to five 18-mer peptides; For S5, I have 14 candidate epitopes corresponding to three 18-mer peptides.

Table 3. Mutations within predicted MHC class I-restricted epitopes

participant	ID	18mer AA sequence	DC1-stimulated IFN-g SFC/10^6	MHC-1 restricted epitope AA sequence	Class 1 restriction	ic50
S4	73-11A	QSSLQTGSEEIKSLYNTV	168	GSEEIKSLY	HLA-A*01:01	47
				SEEIKSLY	HLA-B*44:03	184
				EEIKSLYNTV	HLA-B*44:03	280
				QTGSEEIKSLY	HLA-A*01:01	344
	73-16A	LYCVHQKIEVKDTKEALD	2508	VHQKIEVKDTKEAL	HLA-C*07:01	194
				YCVHQKIEV	HLA-C*12:03	363
	73-24A	QATAATGSSSQNYPIVQNI	1293	QNYPIVQNI	HLA-C*12:03	53
				TAATGSSSQNYPIV	HLA-C*12:03	93
				TAATGSSSQNYPI	HLA-C*12:03	177
				ATAATGSSSQNY	HLA-A*01:01	240
	73-27A	NIQGQMVHQALSPRTLNA	1163	QALSPRTL	HLA-C*12:03	22
				VHQALSPRTL	HLA-C*07:01	36
				MVHQALSPRTL	HLA-C*12:03	120
	73-33A	LKETINEEAAEWDRLHPV	2223	EAAEWDRLHPV	HLA-C*12:03	18
				KETINEEAAEW	HLA-B*44:03	81
				NEEAAEWDRLHPV	HLA-B*18:01	112
				EAAEWDRL	HLA-C*12:03	144

participant	ID	18mer AA sequence	DC1-stimulated IFN-g SFC/10^6	MHC-1 restricted epitope AA sequence	Class 1 restriction	ic50
S5	71-12	QTGSEELKSLYNTVATLY	5607	SLYNTVATLY	HLA-B*15:01	14.67
				SLYNTVATL	HLA-A*02:01	53.76
				SLYNTVATL	HLA-B*15:01	123.55
				KSLYNTVATL	HLA-B*15:01	193.81
				KSLYNTVATL	HLA-A*02:01	196.03
				SLYNTVATL	HLA-C*03:03	242.76
				SEELKSLY	HLA-B*44:02	366.03
	71-13	EELKSLYNTVATLYCVHQ	3525	SLYNTVATLY	HLA-B*15:01	14.67
				SLYNTVATL	HLA-A*02:01	53.76
				SLYNTVATLYCV	HLA-A*02:01	92.08
				SLYNTVATL	HLA-B*15:01	123.55
				KSLYNTVATLYCV	HLA-A*02:01	137.95
				LKSLYNTVATLYCV	HLA-A*02:01	174.61
				YNTVATLYCV	HLA-A*02:01	178.91
				KSLYNTVATL	HLA-B*15:01	193.81
				KSLYNTVATL	HLA-A*02:01	196.03
				SLYNTVATL	HLA-C*03:03	242.76
				SLYNTVATLYCVH	HLA-A*02:01	391.83
				NTVATLYCV	HLA-A*02:01	444.9
	71-14	SLYNTVATLYCVHQRIEV	11087	SLYNTVATLY	HLA-B*15:01	14.67
				SLYNTVATL	HLA-A*02:01	53.76
				SLYNTVATLYCV	HLA-A*02:01	92.08
				SLYNTVATL	HLA-B*15:01	123.55
				YCVHQRIEV	HLA-C*03:03	163.79
				YNTVATLYCV	HLA-A*02:01	178.91
				SLYNTVATL	HLA-C*03:03	242.76
				TLYCVHQRI	HLA-A*02:01	256.91
				TLYCVHQRIEV	HLA-A*02:01	286.98
				SLYNTVATLYCVH	HLA-A*02:01	391.83
				NTVATLYCV	HLA-A*02:01	444.9
				ATLYCVHQRIEV	HLA-A*02:01	453.09

Each table from left to right: 1. Study participant identification number. 2. Name of 18-mers containing predicted autologous variants of MHC class I-restricted epitopes. 3. The amino acid (AA) sequences of 18-mers. The red character indicates the mutation sites.4. The mean IFN-γ response detected in DC-stimulated memory T cells is shown as the number of IFN-γ-producing spot-forming cells per 10^6 responders (IFN-γ SFC/10^6). 5. MHC class I-restriction

for each participant's HLA alleles. 6. IC50nM value for each predicted MHC class I-restricted HIV-1 *gag* epitopes. The predicted output from the algorithm is given in units of IC50nM. A lower number indicates higher affinity.

The viral *gag* sequence alignment also facilitated the identification of the founder sequences (the epitopes in the early stage of infection) for the candidate reservoir epitopes (the epitopes after over years of treatment and viral evolution) for my study participants.

For all the S4 variants, none of them are known epitopes regarding to its HLA restriction; For S5 variants, HLA-A 02:01 SLYNTVATL, which is also well known as epitope SL9, is the only one epitope has been reported according to *Los Alamos CTL/CD8+ T-Cell Epitope Database (https://www.hiv.lanl.gov/content/immunology/ctl_search)*.

Making use of MHC-1 binding predictive algorithm, I compared the IC50nM value of the founder versus reservoir variants (Fig.13). Surprisingly, most IC50nM value of founder epitopes is greater the reservoir variants for S4 (Table 4), which indicates a lower binding affinity between founder epitopes and MHC class I molecule. In other words, the virus mutates to generate an epitope with a greater binding affinity to MHC class I molecule, which are more likely to activate $CD8^+$ T cell.

Table 4. The candidate MHC class I-restricted epitopes for participant S4

<table>
<tr><td>18-mer name</td><td colspan="4">73-11A</td><td colspan="2">73-16A</td><td colspan="4">73-24A</td><td colspan="3">73-27A</td><td colspan="4">73-33A</td></tr>
<tr><td>18mer seq</td><td colspan="4">QSSLQTGSEEIKSLYNTV</td><td colspan="2">LYCVHQKIEVKDTKEALD</td><td colspan="4">QATAATGSSSQNYPIVQNI</td><td colspan="3">NIQGQMVHQALSPRTLNA</td><td colspan="4">LKETINEEAAEWDRLHPV</td></tr>
<tr><td>HLA restriction</td><td>HLA-A*01:01</td><td>HLA-B*44:03</td><td>HLA-B*44:03</td><td>HLA-A*01:01</td><td colspan="2">HLA-C*07:01</td><td>HLA-C*12:03</td><td>HLA-C*12:03</td><td colspan="2">HLA-A*01:01</td><td>HLA-C*12:03</td><td>HLA-C*07:01</td><td>HLA-C*12:03</td><td>HLA-B*44:03</td><td>HLA-C*12:03</td><td>HLA-B*18:01</td><td>HLA-C*12:03</td></tr>
<tr><td>2013 (post-cART)</td><td rowspan="8">GSEEIKSLY (47)</td><td rowspan="8">SEEIKSLY (184)</td><td rowspan="8">EEIKSLYNTV (280)</td><td rowspan="8">QTGSEEIKSLY (344)</td><td colspan="2" rowspan="3">VHQKIEVKDTKEAL(194)</td><td>TAATGSSSQNYPIV (93)</td><td>TAATGSSSQNYPI (177)</td><td colspan="2">ATAATGSSSQNY (240)</td><td rowspan="8">QALSPRTL (22)</td><td rowspan="8">VHQALSPRTL (36)</td><td rowspan="8">MVHQALSPRTL (120)</td><td rowspan="4">KETINEEAAEW (81)</td><td rowspan="4">EAAEWDRLHPV (18)</td><td rowspan="4">NEEAAEWDRLHPV (112)</td><td rowspan="4">EAAEWDRL (144)</td></tr>
<tr><td>1996</td><td>AAATGSSSQNYPIV (31965.50)</td><td>AAATGSSSQNYPI (31582.87)</td><td colspan="2">AAAATGSSSQNY (7269.51)</td></tr>
<tr><td>1993</td><td colspan="3" rowspan="3">AAATGNSSQNYPIV (33385.46)</td><td colspan="2" rowspan="3">AAATGNSSQNYP I(32901.71)</td><td colspan="2" rowspan="3">AAAATGNSSQNY (8899.33)</td></tr>
<tr><td>1992</td><td colspan="2" rowspan="2">VHQKIEVRDTKEAL(37102.69)</td></tr>
<tr><td>1991</td><td rowspan="4">KETINEEAADW (393.3)</td><td rowspan="4">EAADWDRLHPV (19620.55)</td><td rowspan="4">NEEAADWDRLHPV (3738.86)</td><td rowspan="4">EAADWDRL (34673.24)</td></tr>
<tr><td>1989</td><td colspan="2" rowspan="3">VHQKIEVKDTKEAL(194)</td></tr>
<tr><td>1988</td><td>GSEELKSLY (57.31)</td><td>SEELKSLY (439.33)</td><td>EELKSLYNTV (1416.03)</td><td>QTGSEELKSLY (535.75)</td><td rowspan="2">KETINEEAAEW (81)</td><td rowspan="2">EAAEWDRLHPV (18)</td><td rowspan="2">NEEAAEWDRLHPV (112)</td><td rowspan="2">EAAEWDRL (144)</td></tr>
<tr><td>1987</td><td colspan="3">QAISPRTL (21759.67)</td><td>VHQAISPRTL (36550.82)</td><td>MVHQAISPRTL (28409.15)</td></tr>
</table>

First row: name of the five candidate 18-mer peptides. The color in the background is corresponding to the magnitude of IFN-γ response as describe in Fig11. Second row: Sequence of 18-mers. The red character shows where the mutation

has occurred. The blue is new mutation in 2013.Third row: HLA restriction of candidate 18-mer peptides. Forth to eleventh row: sequence of candidate reservoir and founder epitopes. The IC50nM value are shown in the parenthesis below. Variants that have IC50nM value higher than 500nM are highlighted with grey background.

A similar pattern is also recognized for S5 (Table 5). Among the all 14 variants, only the IC50nM value of founder variant **R**S**V**YNTVATL is smaller than its reservoir variant **KSL**YNTVATL, founder variant S**V**YNTVATL is smaller than its reservoir variant S**L**YNTVATL. The rest 12 variants exhibit the same phenomenon as we observed on S4 (Fig.13).

Table 5. **The candidate MHC class I-restricted epitopes for participant S5**

18-mer name	71-12							71-13				71-14		
18mer seq	QTGSEELKSLYNTVATLY							EELKSLYNTVATLYCVHQ				SLYNTVATLYCVHQRIEV		
HLA restriction	HLA-B*15:01	HLA-A*02:01	HLA-B*15:01	HLA-B*15:01	HLA-A*02:01	HLA-C*03:03	HLA-B*44:02	HLA-A*02:01	HLA-A*02:01	HLA-A*02:01	HLA-A*02:01	HLA-C*03:03	HLA-A*02:01	HLA-A*02:01
2013 (post-cART)	SLYNTVATL Y(14.67)	SLYNTVATL (53.76)	SLYNTVATL (123.6)	KSLYNTVAT L(193.8)	KSLYNTVAT L(196)	SLYNTVATL (242.76)	SEELKSLY (366.03)	SLYNTVATLYC V(92.08)	KSLYNTVATLYC V(138)	LKSLYNTVATL YCV(174.6)	SLYNTVATLY CVH(391.83)	YCVHQRIEV (163.79)	TLYCVHQRIEV (286.98)	ATLYCVHQRIE V (453.09)
2002												YCVHQRIEI (56.47)	TLYCVHQRIEI (1141.77)	ATLYCVHQRIEI (1724.08)
2001														
2000												YCVHQRIEV (163.79)	TLYCVHQRIEV (286.98)	ATLYCVHQRIE V (453.09)
1997														
1993														
1990				RSLYNTVATL (79.25)	RSLYNTVATL (288.78)		SEELRSLY (523.97)		RSLYNTVATLYC V (135.89)	LRSLYNTVATLY CV (171.96)		YCVHQRIGV (3743.11)	TLYCVHQRIGV (472.91)	ATLYCVHQRIG V (735.56)
1987	SVYNTVATL Y(28.23)	SVYNTVAT L (589.97)	SVYNTVAT L (372.96)	RSVYNTVAT L (187.1)	RSVYNTVAT L (2896.05)	SVYNTVAT L (94.88)	SEELRSVY (1915.23)	SVYNTVATLYC V (1281.46)	RSVYNTVATLYC V (1794.61)	LRSVYNTVATL YCV (2111.18)	SVYNTVATLY CVH (4479.03)			

First row: name of the five candidate 18-mer peptides. The color in the background is corresponding to the magnitude of IFN-γ response as describe in Fig12. Second row: Sequence of 18-mers. The red character shows where the mutation has occurred. Third row: HLA restriction of candidate 18-mer peptides. Forth to eleventh row: sequence of candidate reservoir and founder epitopes. The IC50nM value are shown in the parenthesis below. Variants that have IC50nM value higher than 500nM are highlighted with grey background.

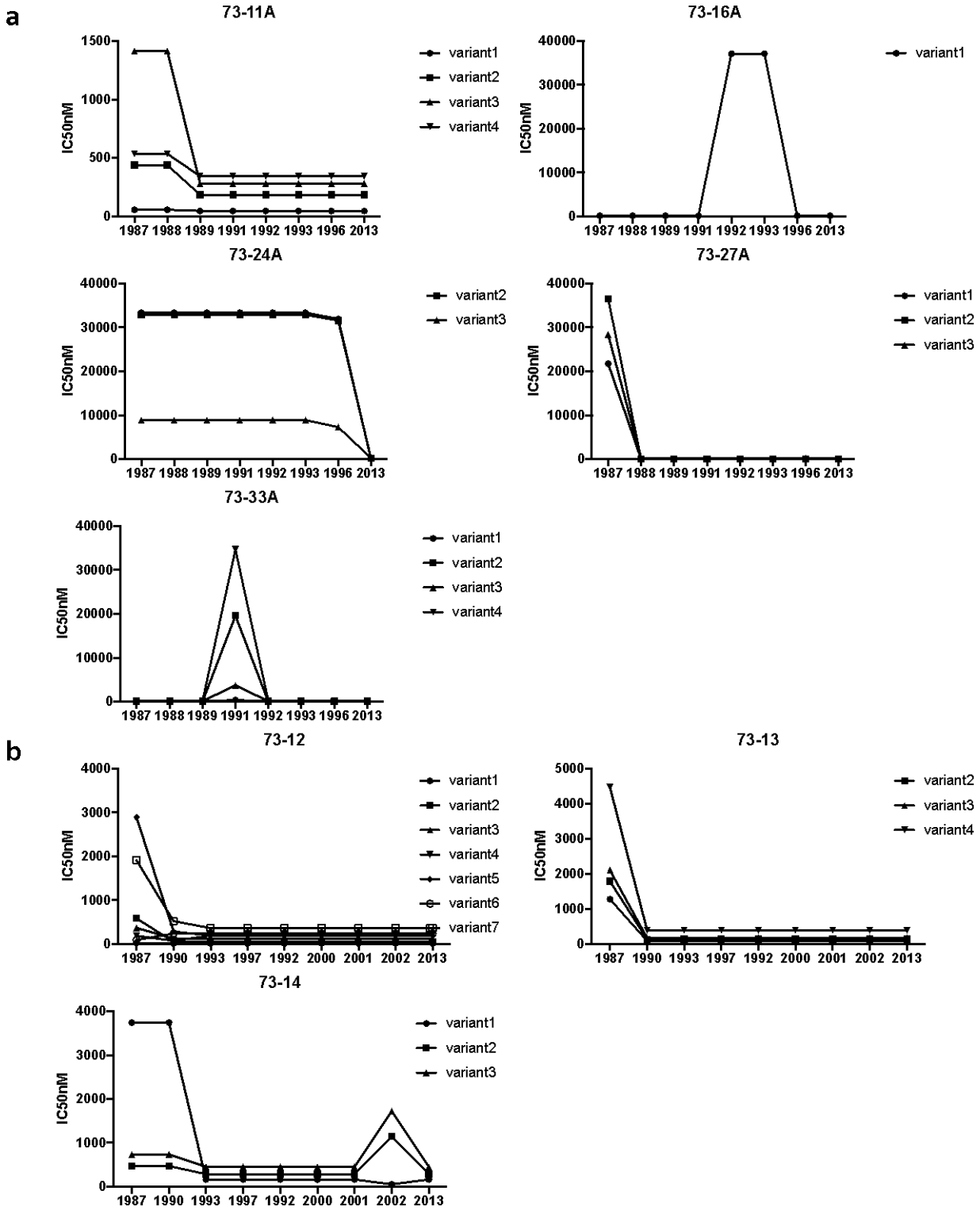

Figure 13. Changes in predicted IC50-nM values for autologous HIV-1 variants over years of viral evolution

a: IC50nM of variants for each S4 18-mer peptide over years.

b: IC50nM of variants for each S5 18-mer peptide over years.

4.7 AN ACCURATE TOOL IS STILL NEEDED TO BE INVENTED TO MONITOR CTL KILLING FUNCTION

CD107a is a degranulation marker of CTL. In order to find an optimal method to monitor CTL killing function, I also utilized a CD107a assay to test the activation of memory CTLs induced by 18-mers (Fig.13). Peptide 73-11A, 73-24A, 73-27A are chosen from the 5 interested mutation-including 18-mer peptides for S4. Peptide 73-57, 73-58 are the S4 18-mer peptides that elicited maximum IFN-γ response based ELISpot assay. Using Flow Cytometry, the peptide 73-57 and 73-58 induced a positive result of CD107a expression. However, 73-11A, 73-24A, 73-27A failed to induce a significant CD107a positive population.

This result confirmed the usage of CD107a as a tool to monitor CTL activation, as the CD107a result is aligned with the result from IFN-γ ELISpot assay. However, it also indicated that the CD107a assay is not sensitive as an IFN-γ ELISpot assay.

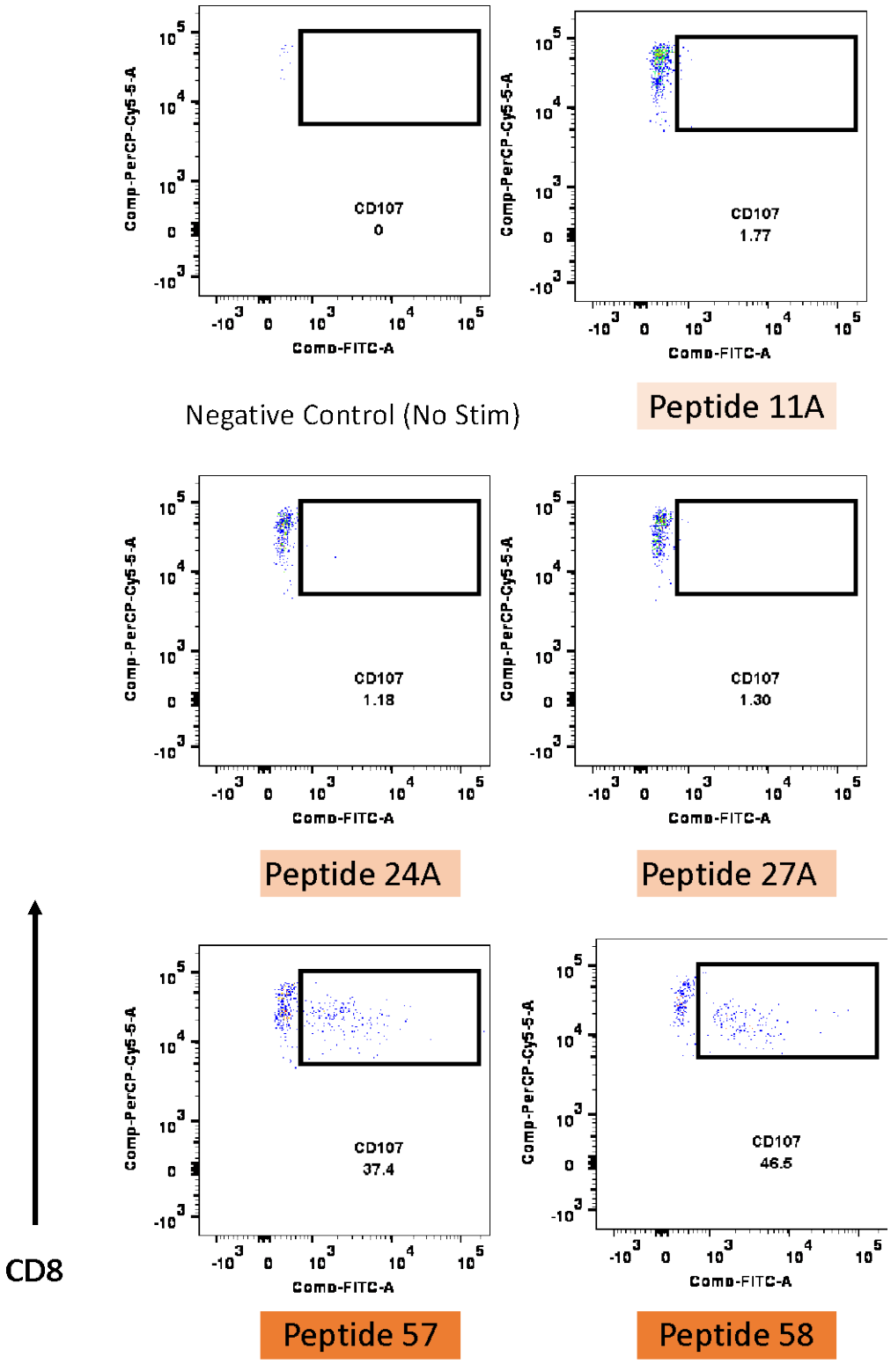
Comp-PerCP-Cy5-5-A
Comb-FITC-A
CD107
0
Negative Control (No Stim)
CD107
1.77
Peptide 11A
CD107
1.18
Peptide 24A
CD107
1.30
Peptide 27A
CD107
37.4
Peptide 57
CD107
46.5
Peptide 58
CD8
CD107a

Figure 14. CD107a assay is less sensitive than IFN-γ ELISpot assay

CD107a expression induced by different 18-mer peptides evaluated by Flow Cytometry. No stim: no stimulation. The color in the background is corresponding to the magnitude of IFN-γ response based on ELISpot as describe in Fig11.

4.8 COMPARISON OF CTL RESPONSE AGAINST FOUNDER AND RESERVOIR VARIANTS USING IFN-γ ELISPOT ASSAY

After having synthetized the S4 candidate peptides, I then tested the CTL response again founder versus reservoir variants using IFN-γ ELISpot assay. To simplify, I chose peptide 73-16A alone for this comparison as it has only one predicted epitope and induced the strongest IFN-γ response among the five interested mutation including 18-mers.

Along years of viral evolution, the viral *gag* sequence had a founder variant VHQKIEV**K**DTKEAL(VKL-16A) from 1987 to 1991. Then it mutated to a reservoir variant peptide VHQKIEV**R**DTKEAL(VRL-16A) at 1992. In 1996, the viral sequence mutated back to its founder variant VKL-16A. According to IEDB predictive algorithm, HLA-C *07:01-restricted peptide VHQKIEV**K**DTKEAL(VKL-16A) has a IC50nM value of 194 and HLA-C *07:01-restricted peptide VHQKIEV**R**DTKEAL(VRL-16A) has a IC50nM value of 37102.69, which indicates VKL-16A has a high binding affinity to MHC class-1 molecule whereas VRL-16A has an extremely low binding affinity. As a result, VKL-16A is capable of recognized by TCR on CTL and induces a high CTL response. However, VRL-16A could not form a MHC-peptide complex to activate CTL. Thus, no IFN-γ response could be detected under VRL-16A stimulation.

Interestingly, both VKL-16A and VRL-16A induced strong CTL response based on a IFN-γ ELISpot assay and no significant different was found in the spots number between these two groups using a p-value of 0.05 (Fig.14).

	IC50nM	IFN-γ ELISpot
Negative control	-	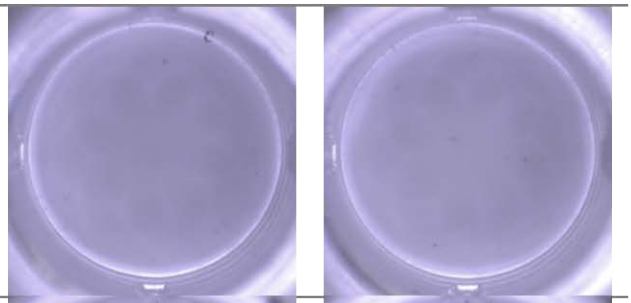
73-16A LYCVHQKIEVKDTKEALD	-	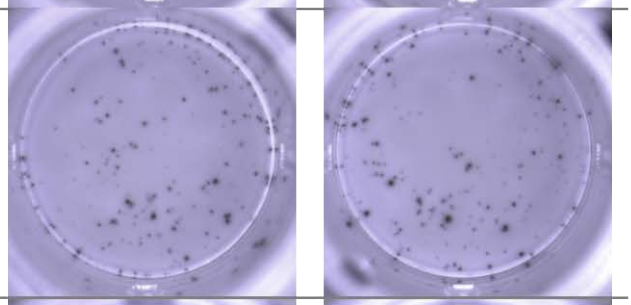
VKL-16A VHQKIEVKDTKEAL	194	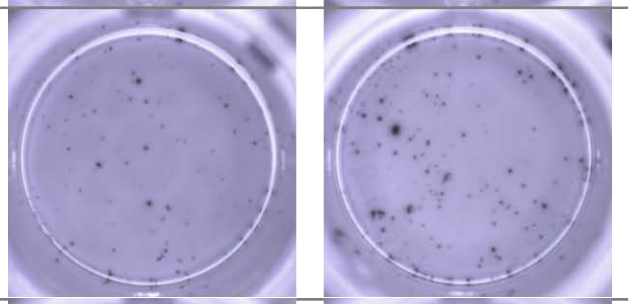
VRL-16A VHQKIEVRDTKEAL	37102.69	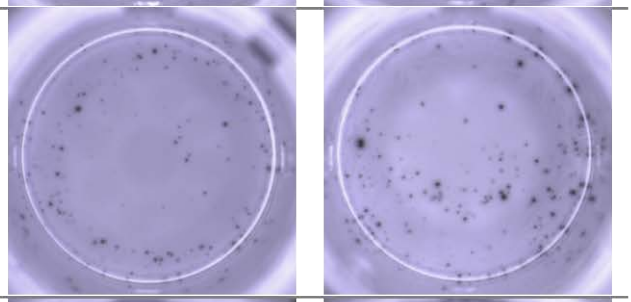
Positive control	-	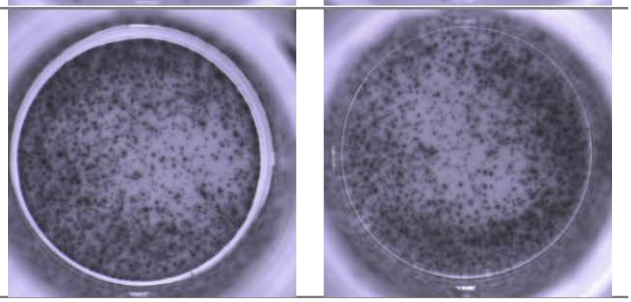

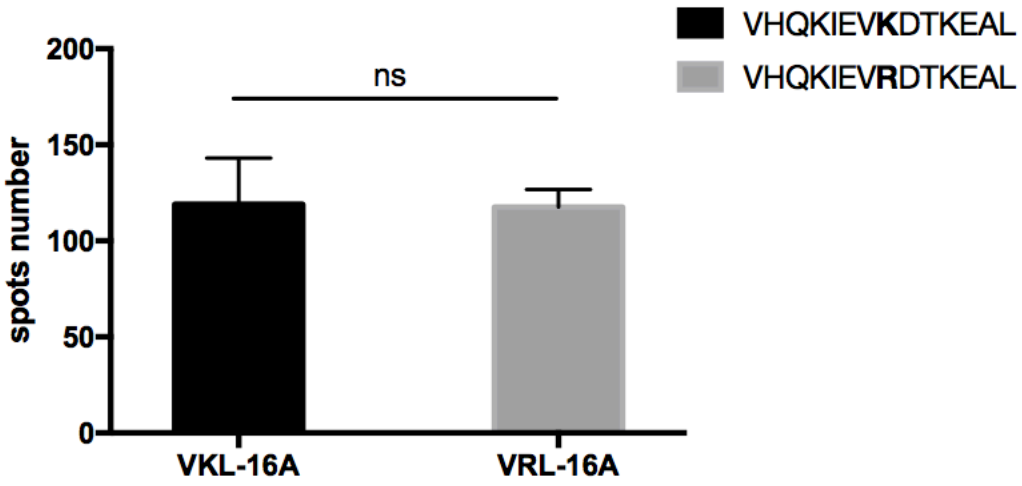

Figure 15. MHC-1 binding affinity does not equal to CTL response

First row of the table: title of each column. Second row of the table: non-stimulation negative control. Third row of the table: IFN-γ response of S4 memory CTL induced by peptide 73-16A. Forth row of the table: IFN-γ response of S4 memory CTL induced by peptide founder variant VKL-16A. Fifth row of the table: IFN-γ response of S4 memory CTL induced by peptide reservoir variant VRL-16A. Sixth row of the table: CD3/CD28 beads positive control.

5.0 DISCUSSION

Combination antiretroviral therapy (cART) is effective in treating chronic HIV infection but fails to completely clear the virus. Mutations in HIV epitopes recognized by CTLs could be a major contributing factor since they result in T cell mediated immune responses with limited effectiveness. However, how these mutations facilities viral escape remains an open question.

To more fully understand the mechanisms of viral pathogenesis and develop effective treatments for HIV-1-infected participants, it is important to identify the epitopes recognized by $CD8^+$ T cells and explore how mutations within epitopes recognized by $CD8^+$ T cells affect HIV-1- specific T cell responses. Here we first set up a peptide library of 18-mers representing the consensus HIV-1 *gag* p17 and p24 sequences for each study participant. Using two different maturation inducing factor cocktails, we generated monocytes into αDC1 and DC2, which are two different types of mature dendritic cells. Using extracellular surface staining, both αDC1 and DC2 were confirmed to have been developed into a fully matured status, though only mature αDC1 is capable of secreting high level of IL-12p70, which was regarded to mediate enhancement of the cytotoxic activity of NK cells and $CD8^+$ cytotoxic T lymphocytes [45, 68]. The mature viral antigen loaded αDC1 and DC2 were then used to stimulate autologous memory $CD8^+$ T cells respectively. After three weeks of stimulation, the memory CTL response was evaluated by IFN-γ ELISpot assay. For study participant S4, there are 28 18mer peptides induced a CTL response that are above the level when processed by αDC1, whereas only 15 when processed by DC2. This indicates that the αDC1 can recognize and process a more broadly range of epitopes than DC2. Having ranked the response compared to the maximum respectively, the magnitude of IFN-γ

response induced by αDC1 is also turned to be stronger compared to the response induced to DC2. On the basis of this finding, αDC1 was chosen as the antigen presenting cell to stimulate memory CTLs in the following experiment. For S5, the monocytes were isolated and matured into αDC1 using the same protocol. Mature αDC1 were then used for autologous $CD8^+$ T cell restimulation. After 21days of co-culture, the 18mers that can induce a positive CTL response were identified using IFN-γ ELISpot.

To locate the epitopes recognized by $CD8^+$ T cell for each study participant, I turned to predictive algorithm provide by *Immune Epitope Database and Analysis Resource* for MHC binding prediction. The algorithm can predict the epitopes as well as its binding affinity to MHC class I molecule. Combining the IFN-γ ELISpot result and the predictive algorithm, I found 99 potential epitopes for S4 and 93 potential epitopes for S5. So far, the epitopes recognized by CTL for both study participants S4 and S5 has been identified successfully.

To identify mutations, I aligned the *gag* p24 and p17 with the span of years. 13 mutations were spotted for both S4 and S5. In order to characterize the memory CTL response to mutated epitopes, I then ruled out all the potential epitopes that with no mutation occurred. Finally, there are 15 candidate epitopes located corresponding to five 18-mer peptides for S4 and 14 candidate epitopes corresponding to three 18-mer peptides for S5. The sequence alignment also facilitated the identification of all the founder and reservoir variants for the candidate epitopes.

To compare the memory CTL response against founder versus reservoir variants, I then collected the value of IC50nM, which is an indicator of MHC class-1 binding affinity, of both founder and reservoir variants. Although there is no direct relationship between the binding affinity and T cell activation, some epitopes do have low affinity, but no known T-cell epitope has an IC50 value greater than 5000nM. The variants mutation could be divided into two groups: 1) For the

variants of S4 peptide 73-16A and 73-33A, the founder epitopes in 1987 has a high MHC class I binding affinity, then it mutates to epitopes with low MHC class I binding affinity. However, over years of viral evolution, the virus mutates back to the sequence with high binding affinity. One possible reason for this phenomenon could be that there is a balance between fitness and immune pressure. When virus mutate to escape immune response, although the mutated *gag* sequence has a lower binding affinity, it could not maintain viral survival. Despite the viruses that have *gag* sequence with high binding affinity are more likely to be recognized by CTLs, they can maintain their survival by fast and efficient replication. This balance between viral survival of immune escape may also explain the continual changes of variants for S5 peptide 71-14; 2) For all the other variants which founder epitopes have a greater IC50nM value, indicating the virus mutates to generate an epitope with a greater binding affinity. The possible explain is that the virus mutates to develop a "baiting" epitopes which have incomplete immune escape from CTL recognition. The subtle modification in viral sequence result in dysfunctional CTLs which could be activated but has lose its killing capacity. When the CTL encounter antigen presenting cells (APC) loaded with "baiting" epitopes, instead of dampening APC as a result of recognition of targets, the CTL provides helper signals to activate the HIV-1 antigen expressing DC, programming them to differentiate into a highly stimulatory, pro-inflammatory type of mature DC. These survived DC rapidly sprout widespread micro- and nanotube-like extensions, allowing them to develop extensive interconnected cellular networks. HIV-1 can utilize such cellular connections for cell-to-cell spread and facilitate *trans* infection of $CD4^+$ T cells [53].

Although ELISpot has been widely used since it was first reported by Sedgwick and Holt in 1983 [69], it has limitations since do not directly measure cytotoxic activity [70]. Moreover, some non-cytotoxic cells can also secrete IFN-γ whereas CTL with proven lytic activity do not

always secrete IFN-γ [71]. There are other protocols in order the measure the cytotoxic activity of $CD8^+$ T cells, including standard ^{51}Chromium (^{51}Cr) release assay [72], which suffer limitations such as hazards associated with radioactivity, cell labeling and high spontaneous; use major histocompatibility complex (MHC) class I tetrameric or pentameric complexes to measure antigen specific $CD8^+$ T cells; assays based on detection of enzymatic activity in target cells including LDH enzyme-release assay [73], Calcein-AM-based Terascan assays [74]. But neither of them measure cytotoxic activity directly [70]. In order to find an optimal protocol to measure memory CTL killing efficacy, I also tried an CD107a assay to test the activation and killing capacity of memory CTLs induced by 18-mer peptides. CTL can mediate cell death by the secretion of cytotoxic molecules including granzymes and perforin. These granzymes and perforin are coated in the granules of cytotoxic effector cells. CD107 is a part of the lipid bilayer surrounding granules. When the CTLs under stimulation, degranulation occurs when microtubules are mobilized and transport the granules toward the synapse between the effector and target cell. Once the granules reach the plasma membrane of the cytotoxic cell, the membranes fusion will allow the lysosome to release the granzymes and perforin, which lead the eventual death of the target cell. Meanwhile, as a consequence of the fusion of lysosomal and cellular membranes during the degranulation process, CD107 are then expressed on the cell surface. With CD107a antibody, this process was assessed using flow cytometry. The antibodies will attach to the surface of effector cell that is expressing CD107 due to degranulation [70]. Although the CD107 assay does not directly measure target cell lysis, it may provide an indication of the cytotoxic potential of the responding $CD8^+$ T cells [75]. Here, S4 peptide 73-11A, 73-24A, 73-27A are chosen from the 15 candidate epitopes. Peptide 73-57 and 73-58 are the potential epitope containing peptides that without mutation but have highest response based on ELISpot result. It turns out that only the cells stimulated by peptide

73-57 and 73-58 induced a significant CD107a positive population after overnight stimulation. This may because CD107a is not as sensitive and accurate as IFN-γ ELISpot assay.

After I had the founder and reservoir variants synthesized, I compared the memory CTL response using IFN-γ ELISpot. The virus had a founder HLA-C *07:01-restricted variant VHQKIEVKDTKEAL(VKL-16A) from 1987 to 1991, and it mutated into a reservoir HLA-C *07:01-restricted variant VHQKIEVRDTKEAL(VRL-16A) in 1992, but then it mutated back to founder variant VKL-16A in 1996. The variant VKL-16A has a IC50nM value of 194 and variant VRL-16A has a IC50nM value of 37102.69. Interestingly, both VKL-16A and VRL-16A induced strong CTL response based on a IFN-γ ELISpot assay and no significant different was found in the spots number between these two groups. This indicates that the predicted IC50nM value for a peptide does not equals to the magnitude of CTL response it would elicited. Another reason could be, as HLA-C restricted variants here, the database is not abundant enough to support an accurate prediction, no matter how well designed the algorithm was.

This thesis provided a basic knowledge for study participant S4 and S5 by having identified the epitopes recognized by $CD8^+$ T cells individually. What's more, by comparing the founder and reservoir variants from HIV-1 chronic infected individuals, different pattern of viral mutation has been observed, indicating a sophisticated mechanism may exist allowing viral escape. An accurate assay for measurement of CTL cytotoxic activity is still required to be developed in the future.

6.0 PUBLIC HEALTH SIGNIFICANCE

HIV has been one of the world's most significant public health challenges for decades. Though cART has shown its effectiveness in the control of the disease progression, it could not lead to a cure of the infection. More importantly, the vast majority of people living with HIV are in low to middle income countries. The high expense of the therapy makes it impossible to have all the patients get proper treatment. As a result, it remains an urgent request to find out the cure to HIV.

The mutated reservoir virus within in the latent cells that evades from host immune response is one of the main obstacles to the cure. It would be possible for us to erase the latent reservoir virus if we could explain the mechanism of viral escape. However, HIV evasion strategy is complicated though several assumptions exist.

This thesis has increased the knowledge of mutated HIV epitopes from contemporaneous viral isolates obtained from long term HIV infected individuals. These data provided basic knowledge of our study participants and showed some clues for the viral evasion strategy, allowing a further study to be continued.

APPENDIX A: SUPPLEMENTARY TABLES

Table 6. The peptide library of 18-mers overlapping by 14 amino acids generated representing the consensus and subdominant HIV-1 *gag* p17 and p24 sequences for S4

GAG	S4 post cART aa consensus sequence		S4 post cART SubDominant clone H9	
p17	73-1A	GKKKYQLKHIVWASRELE		
	73-2A	YQLKHIVWASRELERFAI	73-2B	YQLKHIVWASRELERFAV
	73-3A	HIVWASRELERFAINPGL	73-3B	HIVWASRELERFAVNPGL
	73-4A	ASRELERFAINPGLLETS	73-4B	ASRELERFAVNPGLLETS
	73-5A	LERFAINPGLLETSEGCR	73-5B	LERFAVNPGLLETSEGCR
	73-6A	AINPGLLETSEGCRQILG	73-6B	AVNPGLLETSEGCRQILE
	73-7A	GLLETSEGCRQILGQLQS	73-7B	GLLETSEGCRQILEQLQP
	73-8A	TSEGCRQILGQLQSSLQT	73-8B	TSEGCRQILEQLQPTLQT
	73-9A	CRQILGQLQSSLQTGSEE	73-9B	CRQILEQLQPTLQTGSEE
	73-10A	LGQLQSSLQTGSEEIKSL	73-10B	LEQLQPTLQTGSEEIKSL
	73-11A	QSSLQTGSEEIKSLYNTV	73-11B	QPTLQTGSEEIKSLYNTV
	73-12A	QTGSEEIKSLYNTVATLY		
	73-13A	EEIKSLYNTVATLYCVHQ		
	73-14A	SLYNTVATLYCVHQKIEV		
	73-15A	TVATLYCVHQKIEVKDTK		
	73-16A	LYCVHQKIEVKDTKEALD	73-16B	LYCVHQKIEVKDTKEALE
	73-17A	HQKIEVKDTKEALDKIEE	73-17B	HQKIEVKDTKEALEKIEE
	73-18A	EVKDTKEALDKIEEEQNK	73-18B	*EVKDTKEALEKIEEEQNK*
	73-19A	TKEALDKIEEEQNKSKNK	73-19B	TKEALEKIEEEQNKSKKK
	73-20A	LDKIEEEQNKSKNKAQQA	73-20B	LEKIEEEQNKSKKKAQQA
	73-21A	EEEQNKSKNKAQQATAAT	73-21B	EEEQNKSKKKAQQAAAAT
	73-22A	NKSKNKAQQATAATGSSS	73-22B	NKSKKKAQQAAAATGNSS
	73-23A	QNKAQQATAATGSSSQNYPI	73-23B	QKKAQQAAAATGNSSQNYPI
	73-24A	QATAATGSSSQNYPIVQNI	73-24B	QAAAATGNSSQNYPIVQNI
	73-25A	TGSSSQNYPIVQNIQGQM	73-25B	TGNSSQNYPIVQNIQGQM
p24	73-26A	SQNYPIVQNIQGQMVHQA		
	73-27A	NIQGQMVHQALSPRTLNA		
	73-28A	QMVHQALSPRTLNAWVKV		
	73-29A	QALSPRTLNAWVKVVEEK		
	73-30A	PRTLNAWVKVVEEKAFSP		
	73-21	NAWVKVVEEKAFSPEVIP		
	73-22	KVVEEKAFSPEVIPMFSA		
	73-23	EKAFSPEVIPMFSALSEG		
	73-24	SPEVIPMFSALSEGATPQ		
	73-25	IPMFSALSEGATPQDLNT		
	73-26	SALSEGATPQDLNTMLNT		
	73-27	EGATPQDLNTMLNTVGGH		
	73-28	PQDLNTMLNTVGGHQAAM		
	73-29	NTMLNTVGGHQAAMQMLK		
	73-30	NTVGGHQAAMQMLKETIN		
	73-31	GHQAAMQMLKETINEEAA		
	73-32A	AMQMLKETINEEAAEWDR	73-32B	*AMQMLKETINEEAADWDR*
	73-33A	LKETINEEAAEWDRLHPV	73-33B	*LKETINEEAADWDRLHPV*
	73-34A	INEEAAEWDRLHPVQAGP	73-34B	INEEAADWDRLHPVHAGP
	73-35A	AAEWDRLHPVQAGPVAPG	73-35B	AADWDRLHPVHAGPIAPG
	73-36A	DRLHPVQAGPVAPGQMRE	73-36B	DRLHPVHAGPIAPGQMRE
	73-37A	PVQAGPVAPGQMREPRGS	73-37B	PVHAGPIAPGQMREPRGS
GAG	S4 post cART aa consensus sequence		S4 post cART SubDominant clone H9	
	73-38A	GPVAPGQMREPRGSDIAG	73-38B	GPIAPGQMREPRGSDIAG
	73-39	PGQMREPRGSDIAGTTST		
	73-40	REPRGSDIAGTTSTLQEQ		
	73-41	GSDIAGTTSTLQEQIGWM		
	73-42	AGTTSTLQEQIGWMTNNP		
	73-43	STLQEQIGWMTNNPPIPV		
	73-44	WMTNNPPIPVGEIYKRWI		
	73-45	NPPIPVGEIYKRWIIMGL		

Table 6 Continued

73-46	PVGEIYKRWIIMGLNKIV		
73-47	IYKRWIIMGLNKIVRMYS		
73-48	WIIMGLNKIVRMYSPTSI		
73-49	GLNKIVRMYSPTSILDIK		
73-50	IVRMYSPTSILDIKQGPK		
73-51	YSPTSILDIKQGPKEPFR		
73-52	SILDIKQGPKEPFRDYVD		
73-53	IKQGPKEPFRDYVDRFYK		
73-54	PKEPFRDYVDRFYKTLRA		
73-55	FRDYVDRFYKTLRAEQAS		
73-56	VDRFYKTLRAEQASQEVK		
73-57	YKTLRAEQASQEVKNWMT		
73-58	RAEQASQEVKNWMTETLL		
73-59	ASQEVKNWMTETLLVQNS		
73-60	VKNWMTETLLVQNSNPDC		
73-61	MTETLLVQNSNPDCKTIL		
73-62	LLVQNSNPDCKTILKALG		
73-63A	NSNPDCKTILKALGPGAT	73-63B	NSNPDCKTILKALGPAAT
73-64A	DCKTILKALGPGATLEEM	73-64B	DCKTILKALGPAATLEEM
73-65	ILKALGPGATLEEMMTAC		
73-66A	LGPGATLEEMMTACQGVG	73-66B	LGPAATLEEMMTACQGVG
73-67	ATLEEMMTACQGVGGPGH		
73-68	EMMTACQGVGGPGHKARV		
73-69	ACQGVGGPGHKARVLAEA		
73-70	VGGPGHKARVLAEAMSQV		

Table 7. The peptide library of 18-mers overlapping by 14 amino acids generated representing the consensus HIV-1 *gag* p17 and p24 sequences for S5

GAG		S5 post cART aa consensus sequence
p17	71-1	GRKKYKLKHLVWASRELE
	71-2	YKLKHLVWASRELERFAV
	71-3	HLVWASRELERFAVNPGL
	71-4	ASRELERFAVNPGLLETP
	71-5	LERFAVNPGLLETPEGCR
	71-6	AVNPGLLETPEGCRQILG
	71-7	GLLETPEGCRQILGQLQP
	71-8	TPEGCRQILGQLQPALQT
	71-9	CRQILGQLQPALQTGSEE
	71-10	LGQLQPALQTGSEELKSL
	71-11	QPALQTGSEELKSLYNTV
	71-12	QTGSEELKSLYNTVATLY
	71-13	EELKSLYNTVATLYCVHQ
	71-14	SLYNTVATLYCVHQRIEV
	71-15	TVATLYCVHQRIEVKDTK
	71-16	LYCVHQRIEVKDTKEALD
	71-17	HQRIEVKDTKEALDKIEE
	73-18A	EVKDTKEALDKIEEEQNK
	71-19	TKEALDKIEEEQNKSKKK
	71-20	LDKIEEEQNKSKKKAQQA
	71-21	EEEQNKSKKKAQQAPADT
	71-22	NKSKKKAQQAPADTEKSS
	71-23	QKKAQQAPADTEKSSQVS
	71-23U	QAPADTEKSSQVSQNYPI
	71-24	ADTEKSSQVSQNYPIVQNV
	71-25	SSQVSQNYPIVQNVQGQM
p24	71-26	SQNYPIVQNVQGQMVHQA
	71-27	NVQGQMVHQAISPRTLNA
	71-28	QMVHQAISPRTLNAWVKV
	71-29	QAISPRTLNAWVKVVEEK
	73-30A	PRTLNAWVKVVEEKAFSP
	73-31	NAWVKVVEEKAFSPEVIP
	73-22	KVVEEKAFSPEVIPMFSA
	73-23	EKAFSPEVIPMFSALSEG
	73-24	SPEVIPMFSALSEGATPQ
	73-25	IPMFSALSEGATPQDLNT
	73-26	SALSEGATPQDLNTMLNT
	73-27	EGATPQDLNTMLNTVGGH
	73-28	PQDLNTMLNTVGGHQAAM
	73-29	NTMLNTVGGHQAAMQMLK
	73-30	NTVGGHQAAMQMLKETIN
	73-31	GHQAAMQMLKETINEEAA
	73-32A	AMQMLKETINEEAAEWDR
	73-33A	LKETINEEAAEWDRLHPV
	71-34	INEEAAEWDRLHPVHAGP
	71-35	AAEWDRLHPVHAGPIAPG
	73-36A	DRLHPVQAGPVAPGQMRE
	73-37A	PVQAGPVAPGQMREPRGS
	73-38A	GPVAPGQMREPRGSDIAG
	73-29	PGQMREPRGSDIAGTTST
	73-40	REPRGSDIAGTTSTLQEQ
	73-41	GSDIAGTTSTLQEQIGWM
	71-42	AGTTSTLQEQIGWMTHNP
	71-43	STLQEQIGWMTHNPPIPV
	71-44	WMTHNPPIPVGEIYKRWI
	71-45	NPPIPVGEIYKRWIILGL
	71-46	PVGEIYKRWIILGLNKIV
	71-47	IYKRWIILGLNKIVRMYS
	71-48	WIILGLNKIVRMYSPSSI
	71-49	GLNKIVRMYSPSSILDIK
	71-50	IVRMYSPSSILDIKQGPK
	71-51	YSPSSILDIKQGPKEPFR
	73-52	SILDIKQGPKEPFRDYVD
	73-53	IKQGPKEPFRDYVDRFYK
	73-54	PKEPFRDYVDRFYKTLRA

Table 7 Continued

	73-55	FRDYVDRFYKTLRAEQAS
	73-56	VDRFYKTLRAEQASQEVK
	73-57	YKTLRAEQASQEVKNWMT
	73-58	RAEQASQEVKNWMTETLL
	71-59	ASQEVKNWMTETLLVQNA
GAG		**S5 post cART aa consensus sequence**
	71-60	VKNWMTETLLVQNANPDC
	71-61	MTETLLVQNANPDCKTIL
	71-62	LLVQNANPDCKTILKALG
	71-63	NANPDCKTILKALGPAAT
	73-64A	DCKTILKALGPGATLEEM
	71-65	ILKALGPAATLEEMMTAC
	73-66A	LGPGATLEEMMTACQGVG
	73-67	ATLEEMMTACQGVGGPGH
	73-68	EMMTACQGVGGPGHKARV
	73-69	ACQGVGGPGHKARVLAEA
	73-70	VGGPGHKARVLAEAMSQV
	73-71	GHKARVLAEAMSQVTNSA

APPENDIX B: SUPPLEMENTARY FIGURES

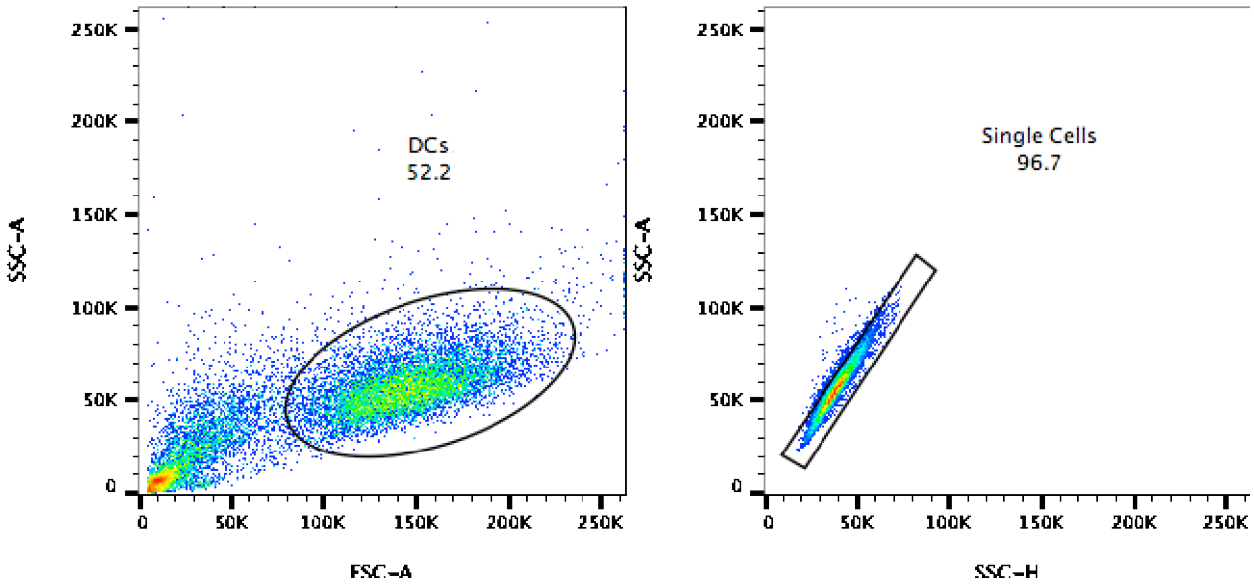

Figure 16. Representative gating strategy used for flow cytometric analyses of αDC1 and DC2 cell surface marker expression levels

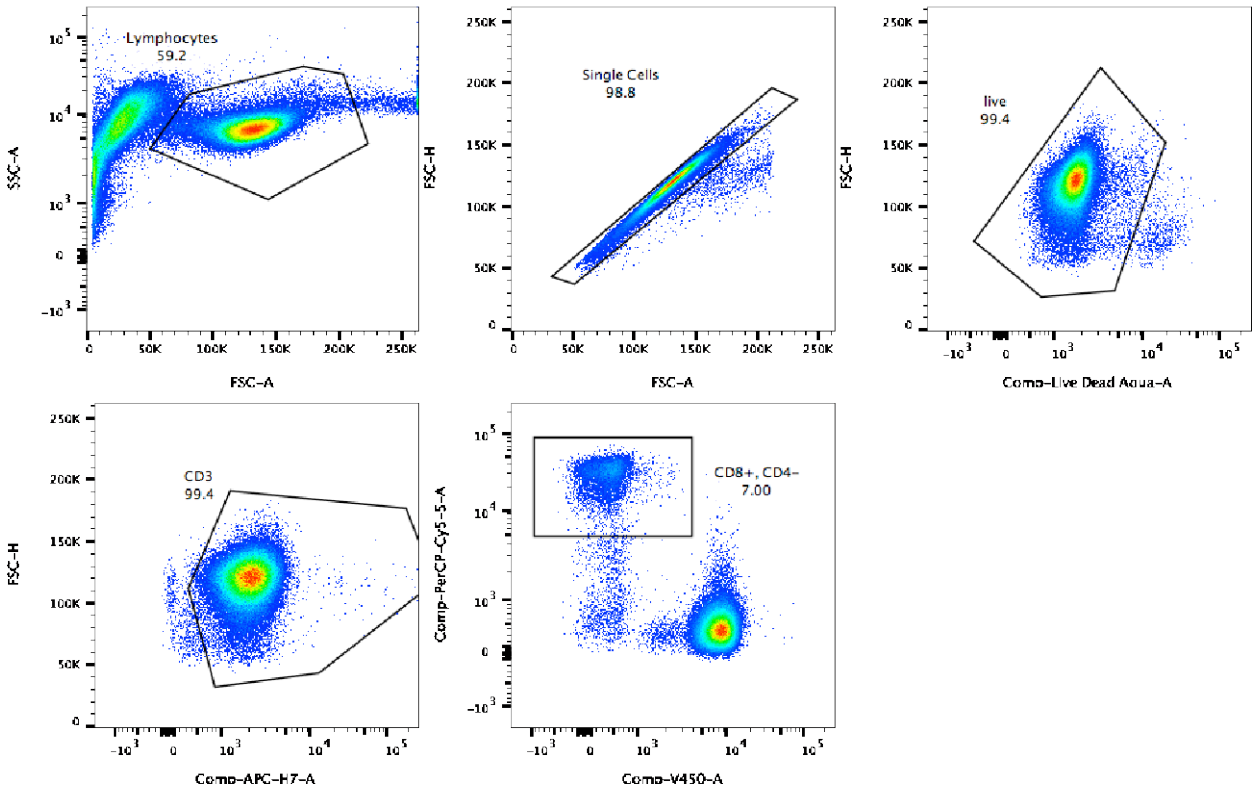

Figure 17. Representative gating strategy used for flow cytometric analyses of CD107a cell surface marker expression levels

BIBLIOGRAPHY

1. Wodarz, D. and M.A. Nowak, *Correlates of cytotoxic T-lymphocyte-mediated virus control: implications for immunosuppressive infections and their treatment.* Philos Trans R Soc Lond B Biol Sci, 2000. **355**(1400): p. 1059-70.
2. Haynes, R.A., 2nd, et al., *Development of a cytotoxic T-cell assay in rabbits to evaluate early immune response to human T-lymphotropic virus type 1 infection.* Viral Immunol, 2009. **22**(6): p. 397-405.
3. Asquith, B., et al., *Inefficient cytotoxic T lymphocyte-mediated killing of HIV-1-infected cells in vivo.* PLoS Biol, 2006. **4**(4): p. e90.
4. Margolis, D.M., et al., *Latency reversal and viral clearance to cure HIV-1.* Science, 2016. **353**(6297): p. aaf6517.
5. Sharp, P.M. and B.H. Hahn, *Origins of HIV and the AIDS pandemic.* Cold Spring Harb Perspect Med, 2011. **1**(1): p. a006841.
6. Reeves, J.D. and R.W. Doms, *Human immunodeficiency virus type 2.* J Gen Virol, 2002. **83**(Pt 6): p. 1253-65.
7. Douek, D.C., M. Roederer, and R.A. Koup, *Emerging concepts in the immunopathogenesis of AIDS.* Annu Rev Med, 2009. **60**: p. 471-84.
8. Sierra, S., B. Kupfer, and R. Kaiser, *Basics of the virology of HIV-1 and its replication.* J Clin Virol, 2005. **34**(4): p. 233-44.
9. Waheed, A.A. and E.O. Freed, *HIV type 1 Gag as a target for antiviral therapy.* AIDS Res Hum Retroviruses, 2012. **28**(1): p. 54-75.
10. Chen, D.Y., et al., *Antiviral activity of human immunodeficiency virus type 1 Gag-specific cytotoxic T lymphocyte targeting is not necessarily intrinsically superior to envelope targeting.* J Virol, 2011. **85**(5): p. 2474-8.
11. Perlmutter, B.L., J.B. Glaser, and S.O. Oyugi, *How to recognize and treat acute HIV syndrome.* Am Fam Physician, 1999. **60**(2): p. 535-42, 545-6.
12. Hightow-Weidman, L.B., et al., *Identifying people with acute HIV infection: demographic features, risk factors, and use of health care among individuals with AHI in North Carolina.* AIDS Behav, 2009. **13**(6): p. 1075-83.
13. Stevenson, M., *HIV-1 pathogenesis.* Nat Med, 2003. **9**(7): p. 853-60.
14. Maartens, G., C. Celum, and S.R. Lewin, *HIV infection: epidemiology, pathogenesis, treatment, and prevention.* Lancet, 2014. **384**(9939): p. 258-71.
15. Portsmouth, S.D. and C.J. Scott, *The renaissance of fixed dose combinations: Combivir.* Ther Clin Risk Manag, 2007. **3**(4): p. 579-83.
16. Trang, T.P., et al., *Drug safety evaluation of oral tenofovir disoproxil fumarate-emtricitabine for pre-exposure prophylaxis for human immunodeficiency virus infection.* Expert Opin Drug Saf, 2016. **15**(9): p. 1287-94.
17. Deeks, S.G., et al., *International AIDS Society global scientific strategy: towards an HIV cure 2016.* Nat Med, 2016. **22**(8): p. 839-50.

18. Finzi, D., et al., *Identification of a reservoir for HIV-1 in patients on highly active antiretroviral therapy.* Science, 1997. **278**(5341): p. 1295-300.
19. Chun, T.W., et al., *Presence of an inducible HIV-1 latent reservoir during highly active antiretroviral therapy.* Proc Natl Acad Sci U S A, 1997. **94**(24): p. 13193-7.
20. Wong, J.K., et al., *Recovery of replication-competent HIV despite prolonged suppression of plasma viremia.* Science, 1997. **278**(5341): p. 1291-5.
21. Chun, T.W., et al., *Quantification of latent tissue reservoirs and total body viral load in HIV-1 infection.* Nature, 1997. **387**(6629): p. 183-8.
22. Marsden, M.D. and J.A. Zack, *Experimental Approaches for Eliminating Latent HIV.* For Immunopathol Dis Therap, 2015. **6**(1-2): p. 91-99.
23. Freer, G. and D. Matteucci, *Influence of dendritic cells on viral pathogenicity.* PLoS Pathog, 2009. **5**(7): p. e1000384.
24. Barroca, P., M. Calado, and J.M. Azevedo-Pereira, *HIV/dendritic cell interaction: consequences in the pathogenesis of HIV infection.* AIDS Rev, 2014. **16**(4): p. 223-35.
25. Cameron, P.U., et al., *Dendritic cells exposed to human immunodeficiency virus type-1 transmit a vigorous cytopathic infection to CD4+ T cells.* Science, 1992. **257**(5068): p. 383-7.
26. Korthals, M., et al., *Monocyte derived dendritic cells generated by IFN-alpha acquire mature dendritic and natural killer cell properties as shown by gene expression analysis.* J Transl Med, 2007. **5**: p. 46.
27. Hashimoto, S.I., et al., *Identification of genes specifically expressed in human activated and mature dendritic cells through serial analysis of gene expression.* Blood, 2000. **96**(6): p. 2206-14.
28. Baltathakis, I., O. Alcantara, and D.H. Boldt, *Expression of different NF-kappaB pathway genes in dendritic cells (DCs) or macrophages assessed by gene expression profiling.* J Cell Biochem, 2001. **83**(2): p. 281-90.
29. Matsunaga, T., et al., *Analysis of gene expression during maturation of immature dendritic cells derived from peripheral blood monocytes.* Scand J Immunol, 2002. **56**(6): p. 593-601.
30. Messmer, D., B. Messmer, and N. Chiorazzi, *The global transcriptional maturation program and stimuli-specific gene expression profiles of human myeloid dendritic cells.* Int Immunol, 2003. **15**(4): p. 491-503.
31. Pereira, S.R., et al., *Changes in the proteomic profile during differentiation and maturation of human monocyte-derived dendritic cells stimulated with granulocyte macrophage colony stimulating factor/interleukin-4 and lipopolysaccharide.* Proteomics, 2005. **5**(5): p. 1186-98.
32. Arico, E., et al., *Immature monocyte derived dendritic cells gene expression profile in response to Virus-Like Particles stimulation.* J Transl Med, 2005. **3**: p. 45.
33. Bleharski, J.R., et al., *Signaling lymphocytic activation molecule is expressed on CD40 ligand-activated dendritic cells and directly augments production of inflammatory cytokines.* J Immunol, 2001. **167**(6): p. 3174-81.
34. Tureci, O., et al., *Cascades of transcriptional induction during dendritic cell maturation revealed by genome-wide expression analysis.* FASEB J, 2003. **17**(8): p. 836-47.
35. Schlaak, J.F., et al., *Cell-type and donor-specific transcriptional responses to interferon-alpha. Use of customized gene arrays.* J Biol Chem, 2002. **277**(51): p. 49428-37.
36. Castiello, L., et al., *Monocyte-derived DC maturation strategies and related pathways: a transcriptional view.* Cancer Immunol Immunother, 2011. **60**(4): p. 457-66.

37. Moschella, F., et al., *Transcript profiling of human dendritic cells maturation-induced under defined culture conditions: comparison of the effects of tumour necrosis factor alpha, soluble CD40 ligand trimer and interferon gamma.* Br J Haematol, 2001. **114**(2): p. 444-57.
38. Jonuleit, H., et al., *Pro-inflammatory cytokines and prostaglandins induce maturation of potent immunostimulatory dendritic cells under fetal calf serum-free conditions.* Eur J Immunol, 1997. **27**(12): p. 3135-42.
39. Jongmans, W., et al., *Th1-polarizing capacity of clinical-grade dendritic cells is triggered by Ribomunyl but is compromised by PGE2: the importance of maturation cocktails.* J Immunother, 2005. **28**(5): p. 480-7.
40. Curtsinger, J.M., D.C. Lins, and M.F. Mescher, *Signal 3 determines tolerance versus full activation of naive CD8 T cells: dissociating proliferation and development of effector function.* J Exp Med, 2003. **197**(9): p. 1141-51.
41. Curtsinger, J.M., et al., *Signal 3 tolerant CD8 T cells degranulate in response to antigen but lack granzyme B to mediate cytolysis.* J Immunol, 2005. **175**(7): p. 4392-9.
42. Mailliard, R.B., et al., *alpha-type-1 polarized dendritic cells: a novel immunization tool with optimized CTL-inducing activity.* Cancer Res, 2004. **64**(17): p. 5934-7.
43. Engell-Noerregaard, L., et al., *Review of clinical studies on dendritic cell-based vaccination of patients with malignant melanoma: assessment of correlation between clinical response and vaccine parameters.* Cancer Immunol Immunother, 2009. **58**(1): p. 1-14.
44. Musey, L., et al., *Cytotoxic-T-cell responses, viral load, and disease progression in early human immunodeficiency virus type 1 infection.* N Engl J Med, 1997. **337**(18): p. 1267-74.
45. Hsieh, C.S., et al., *Development of TH1 CD4+ T cells through IL-12 produced by Listeria-induced macrophages.* Science, 1993. **260**(5107): p. 547-9.
46. Koup, R.A., et al., *Temporal association of cellular immune responses with the initial control of viremia in primary human immunodeficiency virus type 1 syndrome.* J Virol, 1994. **68**(7): p. 4650-5.
47. Goonetilleke, N., et al., *The first T cell response to transmitted/founder virus contributes to the control of acute viremia in HIV-1 infection.* J Exp Med, 2009. **206**(6): p. 1253-72.
48. Phillips, R.E., et al., *Human immunodeficiency virus genetic variation that can escape cytotoxic T cell recognition.* Nature, 1991. **354**(6353): p. 453-9.
49. Allen, T.M., et al., *Selective escape from CD8+ T-cell responses represents a major driving force of human immunodeficiency virus type 1 (HIV-1) sequence diversity and reveals constraints on HIV-1 evolution.* J Virol, 2005. **79**(21): p. 13239-49.
50. Deng, K., et al., *Broad CTL response is required to clear latent HIV-1 due to dominance of escape mutations.* Nature, 2015. **517**(7534): p. 381-5.
51. Goulder, P.J., et al., *Evolution and transmission of stable CTL escape mutations in HIV infection.* Nature, 2001. **412**(6844): p. 334-8.
52. Klenerman, P., Y. Wu, and R. Phillips, *HIV: current opinion in escapology.* Curr Opin Microbiol, 2002. **5**(4): p. 408-13.
53. Mailliard, R.B., et al., *Selective induction of CTL helper rather than killer activity by natural epitope variants promotes dendritic cell-mediated HIV-1 dissemination.* J Immunol, 2013. **191**(5): p. 2570-80.

54. Zaccard, C.R., et al., *CD40L induces functional tunneling nanotube networks exclusively in dendritic cells programmed by mediators of type 1 immunity.* J Immunol, 2015. **194**(3): p. 1047-56.
55. Zaccard, C.R., et al., *HIV's ticket to ride: Cytotoxic T-lymphocyte-activated dendritic cells exploited for virus intercellular transfer.* AIDS Res Hum Retroviruses, 2014. **30**(11): p. 1023-4.
56. Andreatta, M. and M. Nielsen, *Gapped sequence alignment using artificial neural networks: application to the MHC class I system.* Bioinformatics, 2016. **32**(4): p. 511-7.
57. Lundegaard, C., et al., *NetMHC-3.0: accurate web accessible predictions of human, mouse and monkey MHC class I affinities for peptides of length 8-11.* Nucleic Acids Res, 2008. **36**(Web Server issue): p. W509-12.
58. Smith, K.N., et al., *Dendritic cells restore CD8+ T cell reactivity to autologous HIV-1.* J Virol, 2014. **88**(17): p. 9976-90.
59. Kaslow, R.A., et al., *The Multicenter AIDS Cohort Study: rationale, organization, and selected characteristics of the participants.* Am J Epidemiol, 1987. **126**(2): p. 310-8.
60. Shankarappa, R., et al., *Consistent viral evolutionary changes associated with the progression of human immunodeficiency virus type 1 infection.* J Virol, 1999. **73**(12): p. 10489-502.
61. Schenker, E.L., et al., *Evaluation of a dual-color flow cytometry immunophenotyping panel in a multicenter quality assurance program.* Cytometry, 1993. **14**(3): p. 307-17.
62. Giorgi, J.V., et al., *Quality control in the flow cytometric measurement of T-lymphocyte subsets: the multicenter AIDS cohort study experience. The Multicenter AIDS Cohort Study Group.* Clin Immunol Immunopathol, 1990. **55**(2): p. 173-86.
63. Smith, K.N., et al., *Effective Cytotoxic T Lymphocyte Targeting of Persistent HIV-1 during Antiretroviral Therapy Requires Priming of Naive CD8+ T Cells.* MBio, 2016. **7**(3).
64. Rossio, J.L., et al., *Inactivation of human immunodeficiency virus type 1 infectivity with preservation of conformational and functional integrity of virion surface proteins.* J Virol, 1998. **72**(10): p. 7992-8001.
65. Huang, X.L., et al., *Maturation of dendritic cells for enhanced activation of anti-HIV-1 CD8(+) T cell immunity.* J Leukoc Biol, 2008. **83**(6): p. 1530-40.
66. Colleton, B.A., et al., *Primary human immunodeficiency virus type 1-specific CD8+ T-cell responses induced by myeloid dendritic cells.* J Virol, 2009. **83**(12): p. 6288-99.
67. Nielsen, M., et al., *Reliable prediction of T-cell epitopes using neural networks with novel sequence representations.* Protein Sci, 2003. **12**(5): p. 1007-17.
68. Trinchieri, G., *Interleukin-12 and the regulation of innate resistance and adaptive immunity.* Nat Rev Immunol, 2003. **3**(2): p. 133-46.
69. Sedgwick, J.D. and P.G. Holt, *A solid-phase immunoenzymatic technique for the enumeration of specific antibody-secreting cells.* J Immunol Methods, 1983. **57**(1-3): p. 301-9.
70. Shafer-Weaver, K., et al., *The Granzyme B ELISPOT assay: an alternative to the 51Cr-release assay for monitoring cell-mediated cytotoxicity.* J Transl Med, 2003. **1**(1): p. 14.
71. Lehmann, P.V. and W. Zhang, *Unique strengths of ELISPOT for T cell diagnostics.* Methods Mol Biol, 2012. **792**: p. 3-23.
72. Brunner, K.T., et al., *Quantitative assay of the lytic action of immune lymphoid cells on 51-Cr-labelled allogeneic target cells in vitro; inhibition by isoantibody and by drugs.* Immunology, 1968. **14**(2): p. 181-96.

73. Sepp, A., R.M. Binns, and R.I. Lechler, *Improved protocol for colorimetric detection of complement-mediated cytotoxicity based on the measurement of cytoplasmic lactate dehydrogenase activity.* J Immunol Methods, 1996. **196**(2): p. 175-80.
74. Saito, A., et al., *Enhancement of anti-tumor cytotoxicity of expanded gammadelta T Cells by stimulation with monocyte-derived dendritic cells.* J Clin Exp Hematop, 2007. **47**(2): p. 61-72.
75. Betts, M.R., et al., *Sensitive and viable identification of antigen-specific CD8+ T cells by a flow cytometric assay for degranulation.* J Immunol Methods, 2003. **281**(1-2): p. 65-78.